Ore Geology Reviews 84 (2017) 273–288

Contents lists available at ScienceDirect

Ore Geology Reviews

journal homepage: www.elsevier.com/locate/oregeo

Geology, mineralogy, geochemistry and $\delta^{34}S$ of sedimentary rock-hosted Au deposits in Song Hien structure, NE Vietnam

Peter A. Nevolko [a,b,*], Tran Trong Hoa [c], Yury O. Redin [a,b], Tran Tuan Anh [c], Ngo Thi Phuong [c], Vu Hoang Ly [c], Vladislav F. Dultsev [a,b], Pham Thi Dung [c], Ngo Thi Huong [c]

[a] Novosibirsk State University, 2 Pirogova str., 630090 Novosibirsk, Russia
[b] Institute of Geology and Mineralogy, Siberian Branch of the Russian Academy of Sciences, 3 Koptyug ave., 630090 Novosibirsk, Russia
[c] Geological Institute of the Vietnam Academy of Sciences and Technologies, Hanoi, Viet Nam

ARTICLE INFO

Article history:
Received 16 March 2016
Received in revised form 27 December 2016
Accepted 27 December 2016
Available online 19 January 2017

Keywords:
Orogenic gold deposit
Carbonaceous sedimentary rock-hosted gold deposit
Sulfur isotopes
Geochemistry
Song Hien rift
North East Vietnam

ABSTRACT

The Song Hien rift basin is considered to be one of the most important regions of gold mineralisation in North East Vietnam. A number of gold deposits in the Song Hien rift basin are hosted in Triassic and Devonian sedimentary formations of the basin. The largest among them are the Bo Va, Tham Riem and Khung Khoang deposits. The Bo Va deposit is hosted in carbonaceous sedimentary rocks of Triassic age, whereas the Tham Riem and Khung Khoang deposits are hosted in carbonaceous sedimentary rocks of Devonian ages. Based on the mineral composition of the ores, the deposits can be divided into to two types: (i) pyrite dominated and (ii) pyrite-arsenopyrite dominated. The Khung Khoang is of the first type and the Bo Va and Tham Riem deposits belong to the second type. The isotopic composition of pyrite and arsenopyrite in the Tham Riem deposit however, is close to that for the ores of the Bo Va deposit. The $\delta^{34}S$ value for pyrite ranging from −3.7‰ to −7.4‰ and for arsenopyrite ranging from −3.2‰ to 7.4‰. The $\delta^{34}S$ of pyrite in the ore from the Khung Khoang deposit however, has a much heavier isotopic composition of +18.9 to +20.2‰. A narrow range of the variation of sulfur isotopic composition of pyrite and arsenopyrite, the presence of visible gold as inclusions, the presence of chalcopyrite, sphalerite and other inclusions in arsenopyrite and pyrite, the large size of the grains of major ore minerals allow us to assume that the primary gold ores of the Bo Va and Tham Riem deposits underwent metamorphic transformations. The absence of arsenic, antimony, mercury and other characteristic elements in the ores of the Khung Khoang deposit, and substantially heavier isotopic composition of sulfur similar to the sulfur isotopic composition of marine sulfates in the Devonian, allow us to assume another source of the ore components, not connected with the Triassic sedimentary rocks of the Song Hien rift.

1. Introduction

A specific ensemble of precious metals deposits including orogenic gold deposits, Carlin type, and epithermal Au-Sb-Hg mineralization occurs in sedimentary basins containing carbonaceous sediments in many gold provinces of the world (West and Southern Tyan Shan, Eastern Kazakhstan, Verkhoyansk province, the Yenisei Ridge, South-Western China and many others) (Berger et al., 2014; Gold deposits of Russia, 2010; Goldfarb et al., 2014; Goryachev, 2006; Goryachev and Yakubchuk, 2008; Konstantinov et al., 2009; Morelli et al., 2007; Novozhilov and Gavrilov, 1999; Nozhkin et al., 2011; Peters et al., 2007; Spiridonov, 1996; Yakubchuk et al., 2002).

One area that is considered important for metallogenic studies is the Song Hien rift basin in Northeastern Vietnam. The basin consists mainly of Triassic sulfide-rich black shale beds, which play a role as a sedimentary host for various mineral systems such as antimony, mercury and gold-sulfide deposits (Hoa et al., 2008). Gold deposits (of the pyrite-arsenopyrite type) in carbonaceous sedimentary rocks are also known; such deposits include the Bong Mue and Ta Nang ore clusters in Central Vietnam and Southern Vietnam, respectively, as well as the Lang Neo, Lang Vai, Na Pai, Hat Han and other deposits in the northern part of the country (Anh et al., 2015; Hoa et al., 2008; Nguyen, 2008; Tran et al., 2016a,b).

The Triassic Song Hien sedimentary basin extends towards the northwest to the boundary with China and has been interpreted

* Corresponding author at: Institute of Geology and Mineralogy, Siberian Branch of the Russian Academy of Sciences, 3 Koptyug ave., 630090 Novosibirsk, Russia.
E-mail address: nevolko@igm.nsc.ru (P.A. Nevolko).

http://dx.doi.org/10.1016/j.oregeorev.2016.12.032
0169-1368/

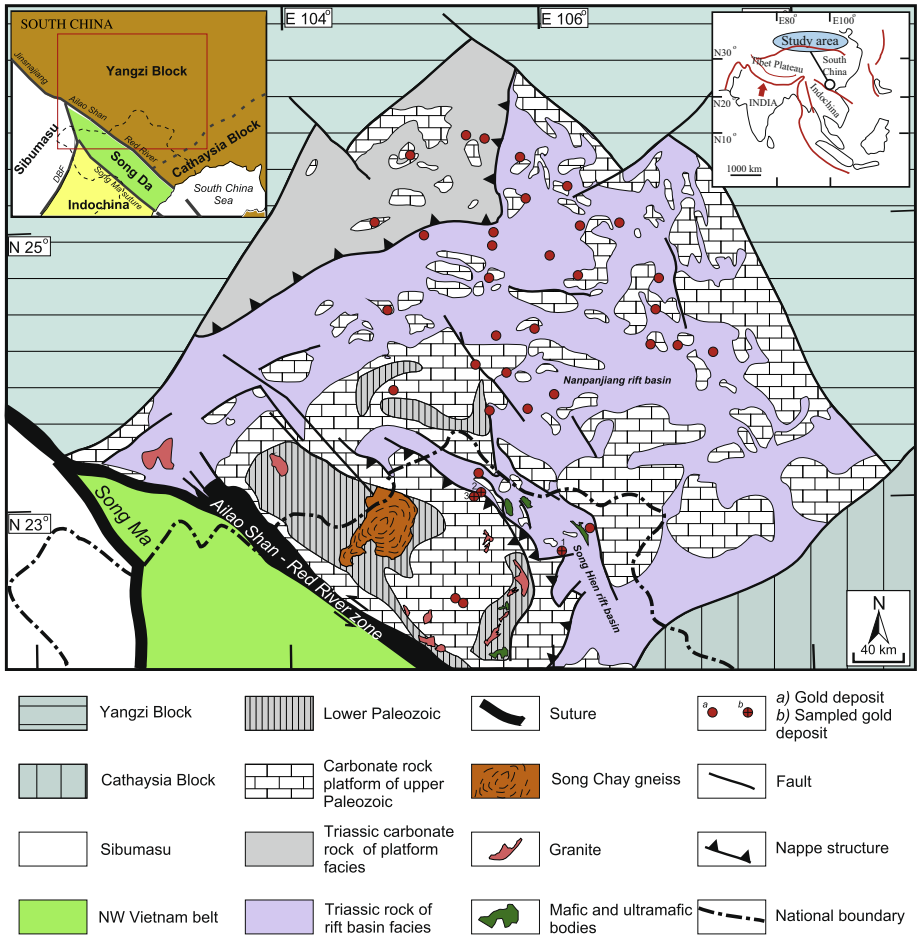

Fig. 1. Regional geological map showing the location of the sampling sites in the gold deposits of Song Hien structure and Yunnan–Guizhou–Guangxi "golden triangle" area (modified from Cai et al., 2014; Chen et al., 2011, 2015a,b; Chen et al., 2014; Lepvrier et al., 2011; Peng et al., 2014; Roger et al., 2012; Svetlitskaya et al., 2015; Yang et al., 2012). *Sampled gold deposit: 1 – Bo Va, 2 – Khung Khoang, 3 –Tham Riem.*

as an intracontinental rift structure related to the Emeishan LIP (Hoa et al., 2008; Izokh et al., 2005; Polyakov et al., 2009; Vladimirov et al., 2012). To the northwest, in the Guangxi and Yunnan provinces of China, the Nanpanjang (Youjiang Basin) sedimentary basin is analogous to the Song Hien (Galfetti et al., 2008; Guangxi BGMR, 1985). Because it hosts a number of gold deposits, Nanpanjang is included in a metallogenic province that is called the "golden triangle" (Chen et al., 2011; Peters et al., 2007; Zhong et al., 2002; Zhou et al., 2002) (Fig. 1).

This paper summarizes the results of investigations in the Song Hien structure that were part of a joint collaborative agreement between the Institute of Geology and Mineralogy (SB RAS) and the Geological Institute (VAST) to study Au deposits hosted in sedimentary rocks in Vietnam. The paper contains descriptions and the results of field and laboratory studies of the Au deposits. In this study, we report for the first time on the ore minerals' compositions, their geochemical characteristics and the sulfur isotopic compositions of the sulfide minerals. We also investigate the relationship between gold mineralization and the tectonic-magmatic evolution of the region.

2. Geological background

2.1. Regional geology

The geological development of South-Eastern Asia began in the Precambrian and continues today. The territory of Vietnam includes parts of two major tectonic blocks (Faure et al., 2014), which are the Indochina Block in the south-west and North Vietnam-South China Block in north-east (Hoa et al., 2008; Zhang et al., 2013). The timing of collision between these blocks is assumed to be mainly Triassic (Lepvrier et al., 1997, 2008, 2011; Liu et al., 2012).

The Red River fault zone is the major structure of northern Vietnam. It is Cenozoic left-lateral shear zone that accommodated the extrusion of Sundaland due to Indian collision (Leloup et al., 1995; Tapponnier et al., 1990;). This zone separates the northern part of the country into two structural tectonic zones – NW and NE fold belts (Faure et al., 2014; Hoa, 2007).

Structural zones or terrains are distinguished within each folded system. The most important structural elements in the north-western part of Vietnam are early Precambrian basement uplifts, which include the Phan Si Pan elevation and the P-T Song Da – Tu Le intracontinental rift system. The structures identified in the north-east include Song Chay Dome, which represents a part of the basement of the Yangzi platform that was remobilized during the Triassic, and the surrounding Lo Gam and Phu Ngu structures that border on the Mesozoic-age Song Hien and An Chau depressions in the east and the arched Yen Minh-Ngan Son fault system in the west (Faure et al., 2014; Hoa et al., 2008; Lepvrier et al., 2011; Tran et al., 2016b).

Terrigenous and volcanogenic-terrigenous Triassic series that are locally interbedded with felsic lavas and their tuffs dominate in the modern erosion section within the Song Hien zone (Faure

et al., 2014). To the north, in the Yunnan and Guangxi provinces of China these sedimentary rocks form a large sedimentary basin known as Nanpanjang (Youjiang Basin) (Galfetti et al., 2008; Guangxi BGMR, 1985), that overlies the Devonian-Carbon-Permian – Early Triassic carbonate platform, which is widespread over the territory of Northern Vietnam and South-Western China. In Northeastern Vietnam, the occurrence of Late Permian bauxite sediments indicates a change in sedimentary regime sedimentation before the formation of the Middle Triassic turbidites (Tri and Vu, 2011). The sedimentation proceeded during two major cycles: (1) During the Late Permian – through the Early Triassic extensional conditions existed during the formation of the rift basin, accompanied by intensive underwater volcanism and formation of carbonaceous sedimentary rocks. (2) During the Middle Triassic cycle of basin development, related to the collision between the Indochina and South China blocks, the sedimentation was characterized by foreland conditions and turbidite formation (Chen et al., 2014; Faure et al., 2014; Tri and Khuc, 2011; Zeng et al., 1995).

The magmatic complexes of the Song Hien structure have been described in detail in many studies (Hoa et al., 2008; Izokh et al., 2005; Roger et al., 2012). The P-T magmatism of the Song Hien structure is characterized by a bimodal volcano-plutonic association in which andesite-basalt and gabbro-dolerite complexes are combined with rhyodacite-rhyolite and granite-granophyric ones (Hoa et al., 2004; Polyakov et al., 1996). Intrusions of ultramafic and mafic composition, namely vehrlites, lherzolites and gabbronorites, are closely associated with basalts and gabbrodolerites. Volcanic picrites comagmatic to gabbronorite-lherzolite intrusives have been also identified. The formation ages of lherzolite, gabbrodolerite and rhyolite, as determined using the U-Pb, zircon, and LA-ICP-MS methods, are 262.3 ± 2.7 Ma, 266.1 ± 3.7 Ma., and 248 ± 4.5 Ma., respectively (Hoa et al., 2008).

Arsenic-rich gold deposits are common in the Song Hien structure. These deposits feature associations between Au, Sb, As, and Hg (Hoa et al., 2008). The largest among them are the Bo Va, Tham Riem and Khung Khoang deposits. Ores of these deposits are hosted within Triassic and Devonian carbonaceous sedimentary rocks. In addition, large antimony deposits are situated in the northern part of Vietnam; among them, the Mau Due deposit is the best studied and described (Ishihara and Pham, 2013).

2.2. Deposit geology

2.2.1. The Bo Va gold deposit

The Bo Va deposit is located at the boundary between the Song Hien rift and the Ngan Son anticline of the Lo Gam folded zone (Fig. 1) and occupies an area of approximately 1.5 km^2. Volcanogenic and terrigenous sedimentary rocks make up the Early Triassic Song Hien formation (Fig. 2). It is separated into two parts (Thanh and Khuc, 2006). (1) The lower part is made up primarily of dark-gray sericitic shale enriched with carbonaceous substances, siltstone and sandstone and is often strongly deformed and interstratified with conglomerates and tuffstone. (2) The upper part is composed of silt-sandstone and shale alternating with sandstone. The total thickness of the lower strata of Song Hien in the region is approximately 250–300 m. According to their lithology, ore-bearing rocks shale, often enriched with carbonaceous matter, quartz-sericite shale, sericitic shale and marl shale. Sulfidized zones with minor pyrite, arsenopyrite and other ore minerals, such as marcasite, ilmenite, and hematite, are often observed in the rocks; they form clusters of fine grains with different concentrations. They are frequently aligned with the schistosity and laminated textures, which often reflect small folds developed during subsequent deformation.

Igneous rocks are a minor component in the region of the Bo Va deposit; only small diabase dykes occur in the south, while biotite granites of Devonian age are located at a distance of 15–20 km to the north-west. Faults extending to the north-west are widely developed; the ore zones are controlled by these faults. They are cut by sub-meridional and north-east extending faults.

Three ore zones are distinguished within the deposit; two of them (the Na Phai 1 and Vi Ba zones) are parallel and extend sub-latitudinally, while the third one (the Na Phai 2 zone) extends to the north-west (Fig. 2.). The extent of ore zones, which consist of a series of closely spaced ore bodies, as determined from the presence of prospecting excavation sites, is about 350–500 m, while their thickness reaches several tens of meters. The dip of the ore bodies is sub-vertical, and the ore bodies often taper out. In general, the ore zones form a united ore field of rather isometric shape with an area of approximately 2 km^2.

There are two types of economic ores. (1) One type is made up of a package of carbonaceous shale with rare occurrences of coarse (up to 1 cm) crystals of arsenopyrite and, to a lesser degree, pyrite. (2) The other type consist of quartz-carbonate veins containing pyrite and arsenopyrite, and smaller amounts of chalcopyrite. The abundance of ore minerals in the ore formations does not exceed several percent.

2.2.2. The Khung Khoang and Tham Riem gold deposits

The Nam Quang ore cluster is situated along the north-western flank of the Song Hien rift structure (Fig. 1) and near a regional fault that separates the trough from the Lo Gam fold belt to the west. The geology of the region in which this deposit occurs is made up of Devonian terrigenous rocks separated into regional stratigraphic formations: Mia Le and Na Quan (Fig. 3). The Mia Le unit is separated into two parts on the basis of its lithologic composition: in the lower one, terrigenous lithologies dominate, including shale, marly shale (which reflects strong sericitic alteration in places) with lenses of limestone and sandy siltstone. These rocks are often enriched with carbonaceous matter. In the upper part Mia Le unit, carbonate rocks dominate, particularly gray limestone with finely interstratified marly and clayey shale. The Na Quan unit contains mainly bituminous limestone. Within the ore cluster, two fault systems are developed in the north-western and sub-parallel directions; they are ore-controlling structures. There is little magmatism in the region of the ore cluster.

There are two deposits within the Nam Quang ore cluster. The Tham Riem and Khung Khoang deposits are located at a distance of 2.5 km from each other (Fig. 3). The ores in both deposits are sulfidized carbonaceous shale and quartz-(carbonate)-sulfide veins. However, there are substantial differences in the ores of these deposits, expressed in terms of differences in their mineral compositions and isotopic characteristics (see below). Gold ore within the Khung Khoang deposit is hosted mainly by pyritized carbonaceous shale, while arsenopyrite is dominant in the Tham Riem deposit. These differences in mineral composition are also reflected in the geochemical characteristics of the mineralization.

2.2.3. Structural settings of the ore bodies

Gold mineralization in the studied deposits may be divided into two structural types, (i) stratiform and (ii) those related to fracture tectonics. Carlin-like gold deposits located to the north, within the territory of Southwestern China, have also been divided into two structural types (Chen et al., 2014).

The Khung Khoang deposit, which contain streaks enriched with gold and sulfide that are concordant with the layered structure of host rocks, belongs to the first type. The thicknesses of these layers vary from several centimeters to several meters. Alternating ore-bearing and ore-free lenses form economically significant gold-bearing bodies. In addition, in many cases the layers enriched

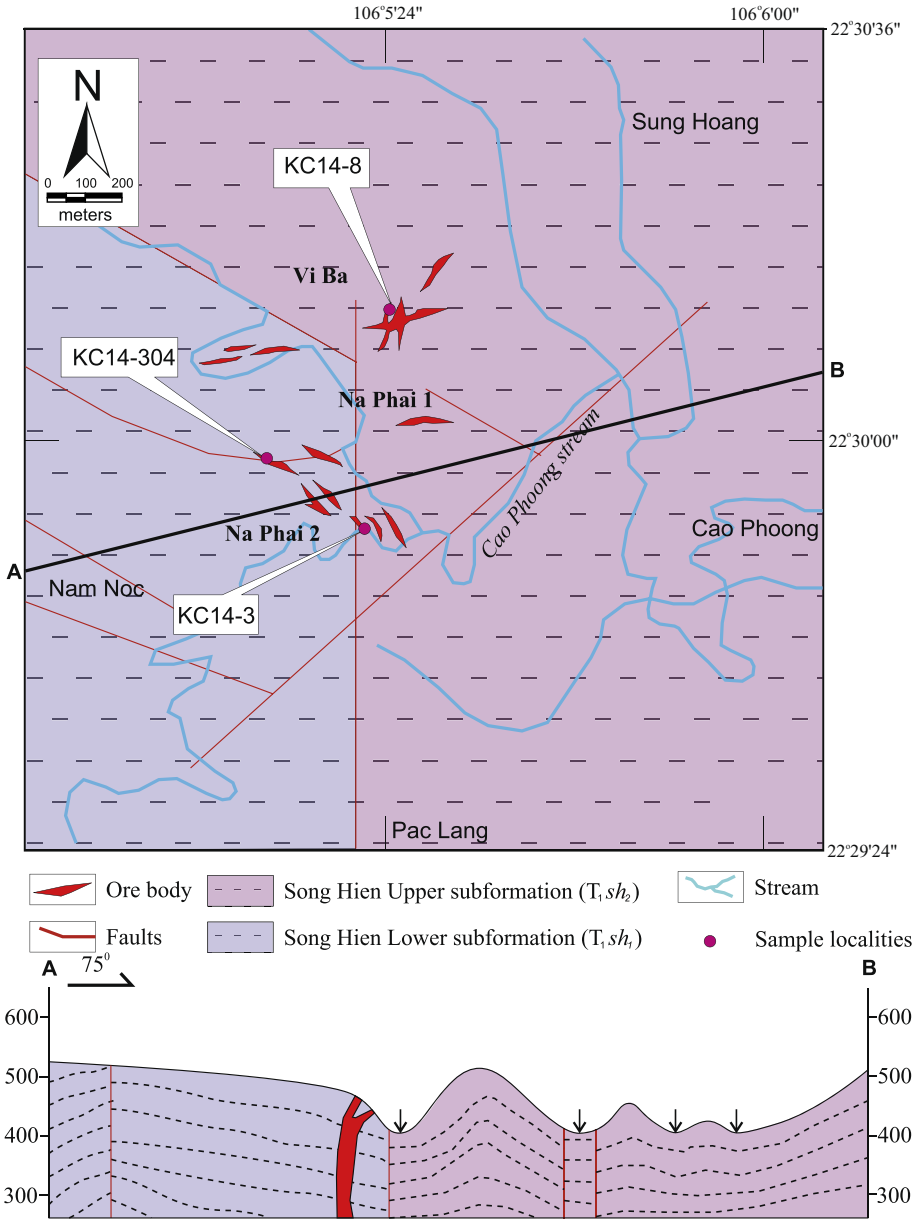

Fig. 2. Geological map and cross section of the Bo Va gold deposit (modified after Petrov et al., 1996).

with sulfides and gold exhibit microfoliation and reflect the folds of the host carbonaceous shale. The maximum degree of sulfidation is confined to the boundary between limestone and carbonaceous shale. In the Bo Va and Tham Riem deposits, ore bodies cross-cut bedding. Sulfidation in these deposits is confined to zones with increased fracturing within the limbs of faults, folds, as well as their hinges.

3. Analytical methods

Samples were collected from ores of the main zone. The mineral composition, textural–structural features, and mineral relations were studied under an optical microscope in reflected and transmitted light. A total of 50 polished sections were studied to characterize the mineralogy, as well as paragenetic and textural relationships. The monomineral fractions of sulfides were sorted under a binocular microscope from heavy concentrates. The chemical composition of sulfides was analyzed in polished samples on a Camebax-micro electron microprobe at the Institute of Geology and Mineralogy in Novosibirsk, Russia. The experimental condition are focused beam in spot mode, accelerating voltage at 20 kV, counting times at 10 s, and beam current at 50 nA. Arsenopyrite and pyrite were analyzed for Fe, S, As, Au, Sb, Ni, Ag, Zn, Cu, and Co. The following sulfides and synthetic composition were used as standards: FeS_2 (Fe, S), FeAsS (As), $Au_{0.75}Ag_{0.25}$ (Au, Ag), Sb_2S_3 (Sb), FeNiCo (Ni, Co), ZnS (Zn), $CuFeS_2$ (Cu). Estimated detection limits were 0.036 wt% for Ni, 0.03 wt% for Co, 0.025 wt% for Fe, 0.05 wt% for As, 0.012 wt% for S, 0.045 wt% for Ag, 0.037 wt% for Sb, and 500 ppm for Au.

The gold content in the sulfides was determined with Perkin-Elmer 3030 Zeeman Atomic Absorption Spectrophotometers (AAS) at the Institute of Geology and Mineralogy, Novosibirsk, Russia. Precision and accuracy were based on the analyses of the standard geological samples SZH-3.

Ag, Cu, Pb, Zn, W, and Tl were analyzed by ICP and ICP-MS (multi-acid digestion), Au, As, Sb, and Hg by INAA (instrumental

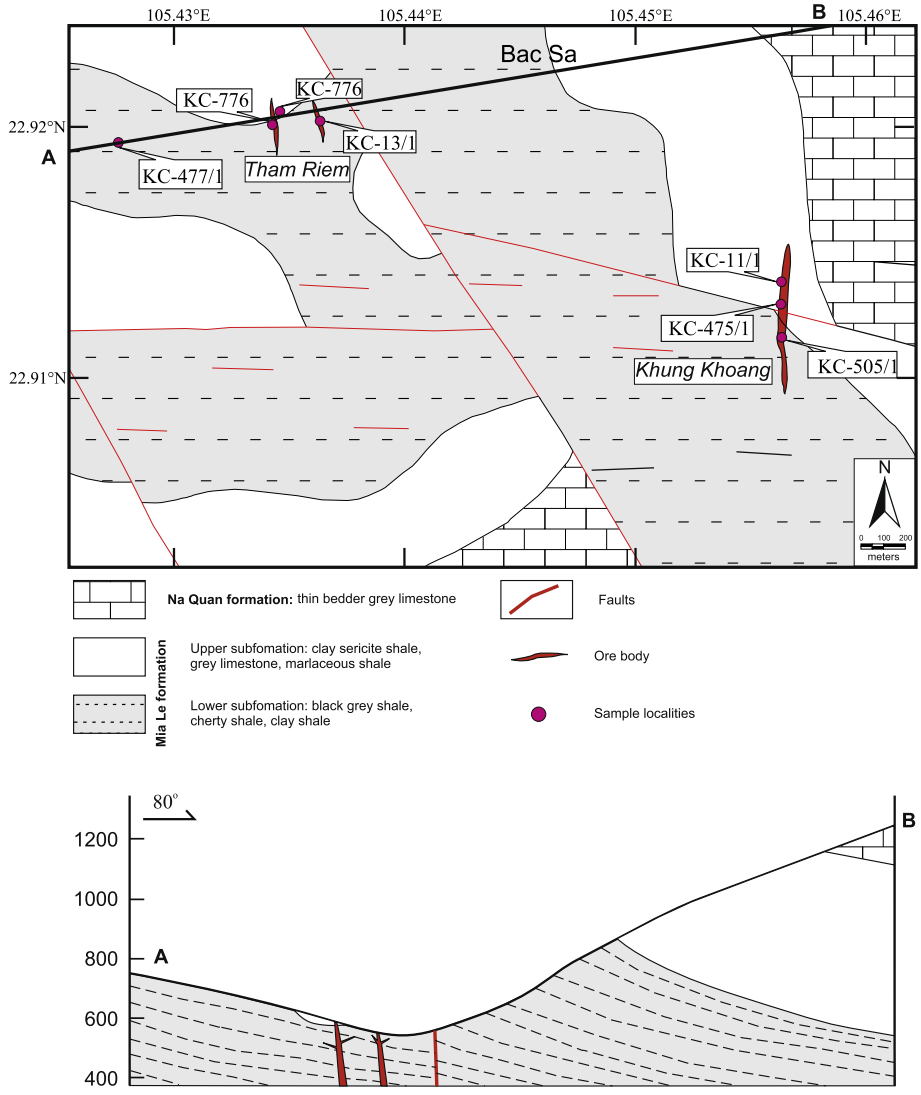

Fig. 3. Geological map and cross section of the Khung Khoang and Tham Riem gold deposits.

neutron activation analysis). Chemical analyses were carried out by Activation Laboratories Ltd, Canada. Detection limit was 1 ppb for Au, 10 ppb for Hg, 0.1 ppm for Sb, 0.2 ppm for Cu, 0.05 ppm for Tl and Ag, 0.5 ppm for As, Pb, and Zn, and 1 ppm for Mo and W.

Sulfur isotope analyses were obtained from twelve samples of pyrite and ten samples of arsenopyrite. Pyrite and arsenopyrite were separated by hand picking under a binocular microscope and the sulfur isotopic ratios were analyzed. The separation of SO_2 from sulfide mineral for sulfur isotopic analysis followed the method proposed by Han et al. (2002). The sulfur isotopic ratios were determined by using a mass spectrometer (Finnigan MAT Delta dual inlet mode) at Institute of Geology and Mineralogy, Siberian Branch, Russia Academy of Science (Novosibirsk). The isotopic composition of sulfur is expressed as $\delta^{34}S$ unit, in permil (‰), relative to Canyon Diablo Troilite standard, and its analytical precision is about ±0.2‰.

4. Mineral composition

4.1. The Bo Va deposit

Three ore lenses are distinguished within the Bo Va deposit, which are the Na Phai 1, Na Phai 2 and Vi Ba lenses. The ores from all three areas are of the same type; they are made up of sulfidized black shale with up to 3–5% sulfide content. In addition, rather thin quartz-carbonate veins with variable thicknesses bearing poor pyrite mineralization occur. In the carbonaceous shales, the sulfides are represented mainly by pyrite and arsenopyrite in approximately equal amounts. Minor minerals include pyrrhotite, chalcopyrite and sphalerite. Large amounts of porphyroblasts of iron carbonate are often observed in the sulfidized carbonaceous shale (Fig. 4b).

Pyrite and arsenopyrite occur in the ores of the Bo Va deposit as coarse idiomorphic phenocrysts (Fig. 5b). Fine pyrite grains often form poor impregnations in carbonaceous shale (Fig. 5a). The sizes of individual grains of ore minerals are 1–3 mm and reach 5–8 mm in some cases (Fig. 4a, b, d). Rare chalcopyrite and sphalerite are confined to the margins of pyrite and arsenopyrite grains, sometimes occupying the intergrain spaces (Fig. 5c, d).

The sulfur content of the analyzed arsenopyrite is higher than that indicated by the stoichiometric composition. Nickel (up to 1.68 mass%) and cobalt (up to 0.8 mass%) occur as trace elements (Table 1). Arsenic content in the analyzed arsenopyrite samples varies within the range 28.76–32.06 at.% (with a mean value of 30.27 at.%). The S/As ratio is within the range 1.09–1.33 (with a

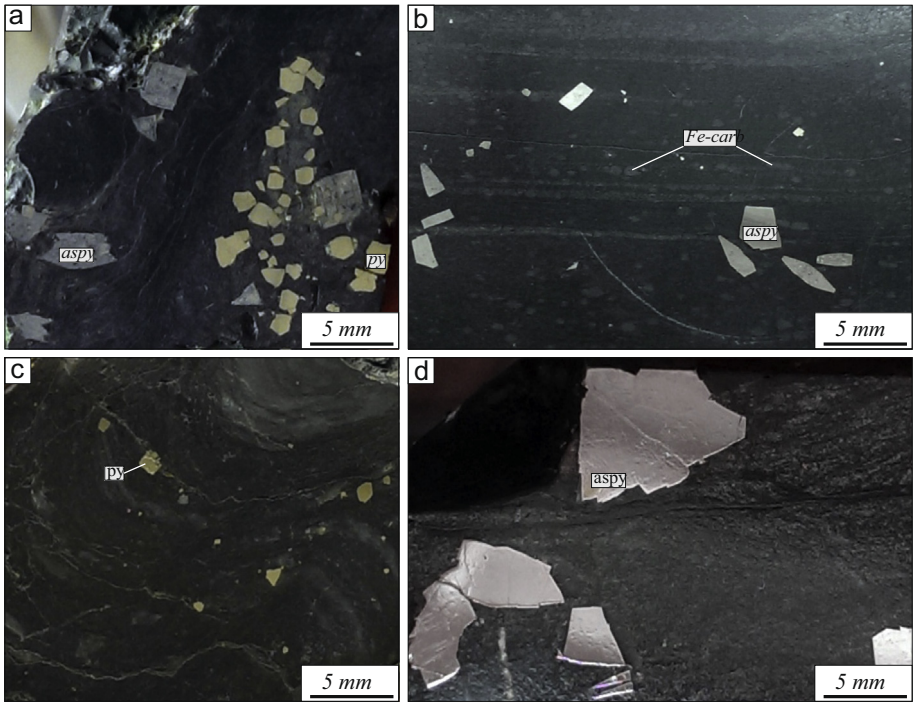

Fig. 4. Reflected light photomicrographs showing the mineral assemblages in black shale in the Bo Va (a, b, d) and Khung Khoang (c) deposits; (a) coarse euhedral arsenopyrite and pyrite; (b) iron-carbonate metamorphic spots or porphyroblasts in gray shale together euhedral arsenopyrite; (c) euhedral pyrite in shale; (d) large euhedral arsenopyrite in gray shale. *Mineral abbreviations*: aspy = arsenopyrite; py = pyrite; Fe-carb = iron-carbonate.

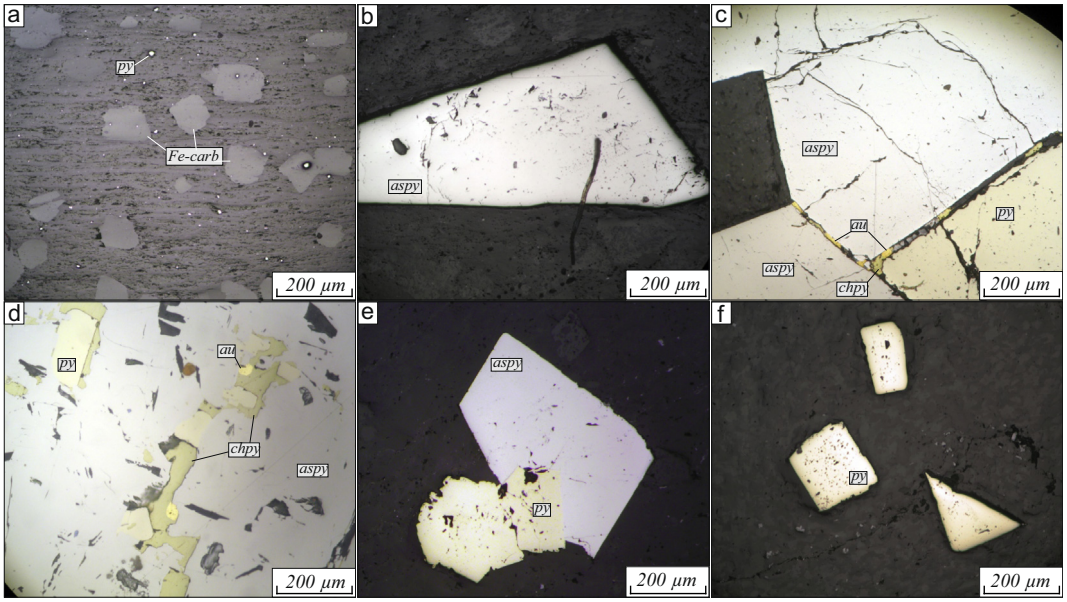

Fig. 5. Photomicrographs showing the characteristics of arsenopyrites and pyrites from the Bo Va (a, b, c, d), Tham Riem (e) and Khung Khoang (f) gold deposits (reflected plane polarized light). (a) minor disseminated pyrite with iron-carbonate metamorphic spots or porphyroblasts in gray shale; (b) coarse euhedral arsenopyrite; (c) small grains of native gold together with chalcopyrite between coarse euhedral arsenopyrite and pyrite; (d) coarse euhedral arsenopyrite containing inclusions of native gold, chalcopyrite and pyrite; (e) euhedral arsenopyrite and pyrite; (f) euhedral pyrite. *Mineral abbreviations*: aspy = arsenopyrite; py = pyrite; au = native gold; chpy = chalcopyrite; Fe-carb = iron-carbonate.

mean value of 1.22). This composition of arsenopyrite is typical of a number of large and unique orogenic gold deposits found in Russia and around the world (Tyukova and Voroshin, 2007).

Pyrite is characterized by its stoichiometric composition (Table 2). As far as trace elements are concerned, in only a few cases arsenic occurs in amounts up to 2.42 mass%, Ni in amounts up to 1.02 mass% and Co in amounts up to 4.32 mass%. The concentrations of other detectable elements do not exceed the detection limit of the microprobe.

Native gold is represented in the ores of the Bo Va deposit by the finest particles 10–50 μm in size. Gold particles are confined to the grains of arsenopyrite and pyrite (Fig 5c, d). The fineness of the native gold of the Bo Va deposit is 850‰ and is due to silver admixture.

Table 1
Electron probe microanalysis results (Au – ppm, other element – wt%) for arsenopyrite from the Bo Va and Tham Riem deposits.

Deposit	Samp. No Detection limit	Ni 0.036	Co 0.030	Fe 0.025	As 0.050	S 0.012	Ag 0.045	Au 500	Sb 0.037	∑
Bo Va	KC14-2	0	0	33.93	44.24	21.44	0	500	0.02	99.68
	KC14-2	0.01	0	34.42	42.49	22.30	0	380	0.01	99.26
	KC14-3/1	0	0	34.58	42.10	22.24	0.01	0	0.01	98.94
	KC14-3/1	0	0	34.52	42.93	21.73	0.01	0	0	99.19
	KC14-3/1	0.01	0	35.04	42.15	22.45	0	0	0	99.66
	KC14-3/2	0	0	34.82	40.84	23.30	0	0	0	98.96
	KC14-3/2	0	0	34.30	43.01	21.47	0	0	0	98.79
	KC14-3/2	0.04	0	34.31	41.88	22.59	0	0	0	98.81
	KC14-8/1	0.01	0	34.76	42.35	22.12	0	0	0	99.23
	KC14-8/1	0	0	34.40	42.64	21.64	0	0	0	98.68
	KC14-8/2	0.14	0.01	34.65	41.92	22.23	0	0	0	98.95
	KC14-8/2	0.03	0	34.77	41.63	22.49	0	0	0	98.91
	KC14-8/2	0	0	35.38	40.95	22.99	0	0	0	99.32
	KC14-8/3	0.20	0.02	34.30	42.72	21.72	0	280	0.05	99.04
	KC14-8/3	0	0	34.51	42.62	22.03	0	390	0.03	99.24
	KC14-8/3	0	0	34.22	43.25	21.42	0.03	380	0.01	98.96
	KC14-8/4	0.01	0	34.52	42.63	22.01	0	0	0.03	99.21
	KC14-8/4	0.06	0	34.84	42.24	22.53	0	0	0	99.67
	KC14-8/4	0.01	0	34.79	42.11	22.19	0	0	0	99.09
	KC14-8/5	0.01	0	34.98	41.93	22.43	0	420	0.02	99.42
	KC14-8/5	0.01	0	34.85	42.24	22.15	0	360	0.07	99.35
	KC14-8/5	0	0	35.19	41.44	23.16	0	340	0.03	99.86
	KC14-304	0	0	34.62	43.18	21.46	0	0	0	99.27
	KC14-304	0.03	0	35.07	42.47	22.55	0	0	0	100.13
	KC14-304	0	0	34.88	41.86	22.56	0	0	0	99.30
	KC14-305	0	0	34.75	42.68	21.71	0	0	0	99.14
	KC14-305	0	0	34.42	43.40	21.74	0.01	0	0.17	99.74
	KC14-305	0.01	0	34.51	43.04	21.70	0	0	0	99.25
	KC14-307	0.01	0	34.83	42.35	22.38	0	0	0.01	99.58
	KC14-307	0.04	0	34.84	42.47	22.00	0	0	0	99.35
	KC14-307	0.06	0	34.73	42.59	21.93	0.01	0	0	99.32
	KC14-314	0.37	0.09	33.91	42.64	22.16	0	350	0.03	99.23
	KC14-314	0.09	0.02	34.77	42.42	22.39	0	660	0.02	99.76
	KC14-314	0.05	0	34.08	43.44	21.67	0.12	280	0	99.38
	KC14-314	0.19	0.06	34.25	43.76	21.76	0	540	0	100.08
	KC14-424	0	0	34.69	44.22	21.56	0	750	0	100.55
	KC14-424	0.18	0.02	34.78	42.81	22.48	0	660	0.02	100.36
	KC14-424	0	0	34.54	44.47	21.19	0	660	0.01	100.27
Tham Riem	KC14-13/3	0.02	0.02	34.41	42.34	22.21	0	0	0.05	99.03
	KC14-13/3	0	0	34.44	42.80	21.67	0	0	0.06	98.97
	KC14-13/3	0	0	34.19	42.95	21.46	0	0	0.02	98.63
	KC14-476/2	0	0	34.18	44.73	20.97	0	400	0.03	100.05
	KC14-476/2	0	0	34.40	44.71	21.07	0	230	0.17	100.38
	KC14-476/2	0	0.02	34.77	44.10	21.40	0	440	0.04	100.38
	KC14-476/2	0	0	34.45	42.51	21.73	0	270	0.32	99.03
	KC14-476/2	0	0	34.48	42.85	21.95	0	440	0.05	99.39
	KC14-476/2	0	0	34.68	43.06	21.95	0	260	0.02	99.73

To determine the level of gold content in the sulfides, atomic absorption analysis was carried out. Arsenopyrite is characterized by levels between 2.2 and 22 ppm, with an average value equal to 7.2 ppm. Similar data were also obtained for pyrite: the average value is 7.3 ppm, with values ranging from 2.5 to 24 ppm.

According to the data from the microprobe analyses, the gold content of the arsenopyrite is below the detection limit. The maximum value obtained in the analyses was 750 ppm, which exceeds the detection limit by 50%. In view of the closeness of the detected concentrations to the lower limit of sensitivity of the procedure the small number of cases in which these values were detected, they cannot be considered reliable. According to the data from the microprobe analyses, the gold content in pyrite does not exceed the lower detection limit under the given conditions.

4.2. The Khung Khoang and Tham Riem deposits

The host rocks in both deposits are represented by carbonaceous shale with different concentrations of ore minerals, and cross-cutting veins containing poor base metal mineralization. The concentrations of ore minerals in sulfidized shales rarely exceeds several percent. The deposits differ in terms of the mineral compositions of the disseminated ores. Arsenopyrite occurs broadly in the ores of the Tham Riem deposit; together with pyrite, it forms disseminated crystals in the total mass of carbonaceous shale, while arsenopyrite was not recognized in the ores of the Khung Khoang deposit. The sizes of individual sulfide grains range from 0.1 to 1 mm.

The mineralogical compositions of the quartz veins crossing the sulfidized shale is similar for both deposits. Ore minerals include pyrite, sphalerite, tetrahedrite, chalcopyrite and native gold. Pyrite in the ores of the Khung Khoang deposit forms rare disseminations with idiomorphic grains up to 1 mm in size (Figs. 4c, 5f). It is characterized by its stoichiometric composition. Only nickel was detected in pyrite by the microprobe. According to a few single analyses, its content reaches 0.19 mass% (Table 2). The concentrations of other detectable elements do not exceed their detection limits. Pyrite in the ores of the Tham Riem deposit is characterized by the stoichiometric composition. Rarely, arsenic is detected in pyrite in the amount up to 0.29 mass%, nickel up to 0.29 mass%,

Table 2
Electron probe microanalysis results (Au – ppm, other element – wt%) for pyrite from the Bo Va, Khung Khoang and Tham Riem deposits.

Deposit	Samp. No Detection limit	Ni 0.036	Co 0.030	Fe 0.025	As 0.050	S 0.012	Ag 0.045	Au 500	Sb 0.037	∑
Bo Va	KC14-2	0.06	0.01	45.94	0	52.65	0	0	0.01	98.67
	KC14-3/1	0.01	0	46.25	0	52.83	0.01	0	0	99.10
	KC14-3/1	0.01	0	46.30	0	53.01	0.01	0	0	99.32
	KC14-3/2	0	0	45.72	0	54.02	0	0	0	99.74
	KC14-3/2	0.34	0.21	45.14	0.59	52.83	0	0	0	99.11
	KC14-8/1	0.21	0	46.02	0	52.86	0	0	0	99.08
	KC14-8/1	0.03	0	46.21	0	53.28	0.01	0	0	99.54
	KC14-8/2	0	0	45.87	1.08	52.62	0	0	0	99.57
	KC14-8/2	0.02	0	46.52	0	53.60	0	0	0	100.14
	KC14-8/3	0.38	4.32	44.64	0	51.51	0.02	0	0	100.87
	KC14-8/4	0.01	0	46.67	0	53.07	0.01	0	0	99.76
	KC14-8/4	0.24	0.01	46.25	0.02	52.77	0	0	0	99.28
	KC14-8/5	0	0	45.95	0	52.66	0.01	0	0	98.62
	KC14-8/5	0.02	0	46.29	0	52.33	0	0	0.02	98.67
	KC14-304	0.02	0	45.52	1.75	51.91	0	0	0.03	99.23
	KC14-304	0.01	0	46.02	0	52.97	0.01	0	0	99.01
	KC14-304	0.01	0	46.45	0	53.17	0	0	0	99.63
	KC14-305	0.01	0	46.28	1.09	52.33	0	0	0	99.70
	KC14-305	0.04	0	46.06	0	53.42	0	0	0	99.52
	KC14-307	0.05	0	46.64	0	52.98	0	0	0	99.67
	KC14-307	0.05	0	46.39	0	52.70	0.01	0	0	99.16
	KC14-307	0.02	0	46.47	0	52.53	0	0	0	99.02
	KC14-408	0.09	0.04	46.34	0	52.95	0.01	0	0.01	99.45
	KC14-408	0.10	0	45.85	0	53.74	0	0	0	99.69
	KC14-408	0.20	0.10	45.42	0	53.75	0.02	0	0	99.52
Tham Riem	KC14-13/1	0	0	46.60	0	52.77	0	0	0.01	99.38
	KC14-13/1	0.07	0	46.24	0	52.38	0	0	0	98.69
	KC14-13/1	0	0	46.81	0	52.22	0.03	0	0.01	99.07
	KC14-13/1	0	0	46.18	0	52.54	0	0	0.01	98.73
	KC14-13/3	0.03	0.05	46.15	0	52.74	0	100	0	98.97
	KC14-13/3	0.05	0.01	45.85	0	52.28	0	230	0	98.21
	KC14-13/4	0.12	0	46.48	0	53.04	0.01	0	0.02	99.67
	KC14-13/4	0.14	0.27	46.10	0	53.05	0	0	0	99.55
	KC14-13/4	0.07	0	46.42	0	52.85	0.04	0	0.01	99.38
	KC14-13/4	0.08	0	46.07	0	53.29	0.02	0	0.01	99.48
	KC14-320/2	0.03	0.44	45.62	0	52.99	0	0	0.03	99.11
	KC14-320/2	0.10	0	45.67	0	53.00	0	0	0.03	98.80
	KC14-320/2	0.04	0.50	45.35	0	52.59	0	0	0.01	98.48
Khung Khoang	KC14-12/1	0	0	46.00	0	53.00	0.01	0	0	99.00
	KC14-12/1	0	0	46.22	0	53.02	0	180	0	99.27
	KC14-12/1	0.08	0	45.92	0	52.88	0	0	0	98.88
	KC14-12/1	0.01	0	46.21	0	53.07	0	0	0	99.28
	KC14-12/3	0	0	46.48	0	53.11	0	0	0	99.60
	KC14-12/3	0	0	46.19	0	53.34	0	0	0.01	99.54
	KC14-12/3	0.19	0.06	45.87	0	53.16	0	0	0	99.28
	KC14-12/3	0.02	0	46.24	0	52.91	0.02	0	0.03	99.22
	KC14-12/3	0.02	0	46.06	0	52.71	0.01	0	0.01	98.80

and cobalt up to 0.5 mass% (Table 2). The concentrations of other detectable elements do not exceed the microprobe detection limit.

There is less arsenopyrite than pyrite in the Tham Riem deposit. Almost everywhere pyrite and arsenopyrite occurs in intergrowths (Fig. 5e). Trace elements in significant amounts were not detected in the arsenopyrite. The arsenic content in the analyzed arsenopyrite samples varied within the range of 29.5–30.9 at.% (with a mean value of 30.3 at.%). The S/As ratio is within the range 1.16–1.27 (with a mean value of 1.21) (Table 1).

Native gold was found in the form of fine inclusions in pyrite and more rarely in arsenopyrite. In addition to pyrite, native gold forms intergrowth with pyrite, chalcopyrite and tetrahedrite in quartz veins. The sizes of native gold grains are 10–40 μm. Only silver is present in the native gold as a trace element at an abundance of 1.2–8.6 mass%. The average fineness of the native gold is 950‰.

Pyrite and arsenopyrite in the ores from the Khung Khoang and Tham Riem deposits do not contain significant concentrations of gold. According to data from AAS analyses, the average gold content in the sulfides is 2.7 ppm. Determination of mineral compositions by the EPMA method did not reveal significant (above the detection limit) gold content in pyrite or arsenopyrite (Tables 1 and 2).

4.3. Mineral types of gold ore

Our studies showed that the mineral parageneses of the gold deposits are rather simple. The major ore minerals connected with gold mineralization are arsenopyrite and pyrite.

Based on the mineralogical compositions of the ores, we divide the studied deposits into two types: (i) pyrite and (ii) pyrite-arsenopyrite. The first type includes the Khung Khoang deposit, in which pyrite is the only ore mineral. The average size of the pyrite grains is 0.1 mm, and they form enriched layers in carbonaceous shale. An essential difference in the pyrite from the Khung Khoang deposit relative to other similar deposits (orogenic sedimentary hosted arsenopyrite-free deposits, for example the Suhoi Log deposit (Large et al., 2011; Yudovskaya et al., 2016)) is the absence of arsenic in the composition of the pyrite.

The Bo Va and Tham Riem deposits belong to the pyrite-arsenopyrite type. The ores of these deposits are characterized by extensive dissemination with coarse idiomorphic grains of pyrite and arsenopyrite. The quantitative relations between the two major ore minerals may vary within the limits of each ore body but remain constant of the scale of the whole deposit. Rare and minor minerals include chalcopyrite, sphalerite, and native gold.

For this ore type, some features may be identified that distinguish them from the ores of classical deposits in carbonaceous rocks, as well as the Carlin-like deposits in the territory of Southern China (Chen et al., 2011; Peters et al., 2007; Zhong et al., 2002; Zhou et al., 2002): (a) very limited amounts of ore minerals, the absence of minerals containing antimony and mercury, as well as low-temperature realgar and orpiment; (b) low gold content in the iron sulfides; (c) the occurrence of visible native gold in the form of inclusions in pyrite and arsenopyrite. These features of gold mineralization are the main differences compared to the Carlin-like deposits situated in the southern part of China.

5. Geochemical and sulfur isotopic composition

The Au, As, Sb association is typical for the gold deposits in carbonaceous sedimentary rocks (Novozhilov and Gavrilov, 1999). The most important geochemical feature of this mineralization type is a clearly pronounced correlation of gold with arsenic, and more rarely with antimony. For the Carlin type deposits in Nevada, and in the south-west of China, the association Au, As, Sb, Hg, Tl is typical (Chen et al., 2011; Peters et al., 2007; Zhang et al., 2005). In order to reveal the geochemical signature of gold mineralization, and strength of correlation between gold and trace elements in ores, ICP-MS and INAA analyses were carried out at the LTD Laboratory (Ontario, Canada).

5.1. The Bo Va deposit

The gold content in the ores of the Bo Va deposit is not high (up to 2–5 ppm). The Au/Ag ratio is within the range of 2–0.5. The ores of the Bo Va deposit are characterized by a rather small set of trace elements. Only arsenic is characterized by anomalously high concentrations. Its content in some samples reaches several percent. The contents of antimony and mercury are up to 30 and 10 ppm, respectively (Table 3).

To reveal gold correlation with other trace elements, we carried out correlation analysis of the ICP analyses. Fig. 6 shows a positive correlation between Au and S concentration.

5.2. The Khung Khoang and Tham Riem deposits

The gold content in the ores of the Khung Khoang and Tham Riem deposits is rather low, not more than 1.5–2 ppm. According to the mineral composition of the ores, three ore types may be distinguished: (i) carbonaceous shales with pyrite-arsenopyrite mineralization (Tham Riem deposit), (ii) carbonaceous shales with pyrite mineralization (Khung Khoang deposit), and (iii) quartz veins with tetrahedrite – sphalerite mineralization (Tham Riem and Khung Khoang deposits). Each of these types is characterized by a specific set of trace elements.

Carbonaceous shales with pyrite-arsenopyrite mineralization occurring in the Tham Riem deposit contain up to 1.5–2 ppm gold. The silver content rarely reaches 2 ppm. The Au/Ag ratio is close to 1. Only arsenic is characterized by anomalously high concentrations, which reach 5000 ppm. Relatively increased concentration of Sb (up 50 ppm), Hg (up to 3 ppm) and Se (up to 32 ppm) are present in the ores (Table 3). The concentrations of other elements do not exceed the clarke level by more than one order of magnitude, or are at the clarke level. The correlations between gold and other trace elements reveal a constant positive correlation with arsenic. No correlations were detected between the increased gold content and other ore elements.

The pyritized carbonaceous shales of the Khung Khoang deposit are characterized by low gold and silver contents that are not higher than 1 ppm. The arsenic concentration in the ores reaches 400 ppm. The concentration of Sb is relatively increased – up to 25 ppm (Table 3). The other elements do not substantially exceed their clarke values.

Table 3
Gold and accessory elements concentration of ores from the Bo Va, Khung Khoang and Tham Riem deposits.

Deposit	Samp. No	Analyte Symbol Unit Symbol Detection Limit	Au ppb 1	Ag ppm 0.05	As ppm 0.5	Sb ppm 0.1	Hg ppb 10	Tl ppm 0.05	Pb ppm 0.5	Zn ppm 0.5	Cu ppm 0.2	Mo ppm 1	W ppm 1
Bo Va	KC14-3/1		197	0.38	4160	12.4	10	1.7	10.3	100	60.9	0.4	1
	KC14-8/1		23	0.99	227	10.6	60	1.77	9.7	155	40.5	0.2	1
	KC14-8/2		1280	1.29	29,700	0.7	10	1.87	44.7	48.6	39.2	0.3	1
	KC14-8/3		854	0.47	35,200	0.7	60	1.09	9.6	14.2	12.1	0.4	1
	KC14-307		100	0.44	4990	10.6	10	1.72	5.7	104	68.2	0.5	1
	KC14-407/1		2170	1.99	6550	15.8	9100	2.37	35.4	78.4	147	1	1
	KC14-407/2		711	1.51	4130	13.2	7020	2.65	18.6	43.4	38.3	2	1
	KC14-408		132	1.22	279	15.1	10,000	1.65	21.7	103	142	1	1
	KC14-414		286	0.86	5000	13.8	10,000	2.02	14.1	59.6	73.2	1	1
	KC14-424		226	0.84	7700	23.3	10,000	2.3	12.4	61.3	57.9	1	1
	KC14-433		1030	0.95	16,800	36.1	10,000	2.58	30.4	41.1	84.5	3	1
Khung Khoang	KC14-12/1		200	0.5	120	24.6	80	1.16	21.3	119	26.2	1.9	1
	KC14-12/2		32	0.17	403	16.6	10	0.52	17.4	25.3	7.6	1.1	1
	KC14-475/2		122	0.36	146	24.6	2400	0.38	53.4	49.1	31.3	2	1
	KC14-475/5		701	0.96	154	47	1340	1.42	38	72.1	48.3	1	1
	*KC14-319/1**		*45*	*3.01*	*131*	*420*	*1600*	*0.14*	*6.5*	*2910*	*653*	*1.7*	*1*
Tham Riem	KC14-13/3		891	0.42	2650	30.9	60	1.52	14.5	136	32.7	0.7	1
	KC14-320/1		1290	0.43	5230	48.5	60	1.93	45.2	160	48	0.7	1
	KC14-476/1		60	0.98	57.2	13	3000	0.1	9.8	53.2	15.9	1	1
	KC14-476/2		76	1.17	169	38.8	2220	1.24	22.4	207	83.2	5	1
	*KC14-320/2**		*132*	*2.87*	*80.4*	*495*	*540*	*0.05*	*545*	*1320*	*705*	*0.2*	*1*
Host rock**	KC14-477/2		61	1.99	48.2	28.2	2230	1.16	14.5	72	29.4	9	1

Note: * – quartz-sulfide vein; ** – host rock – black shale from outcrop near the Tham Riem deposit (see location sample in Fig. 3).

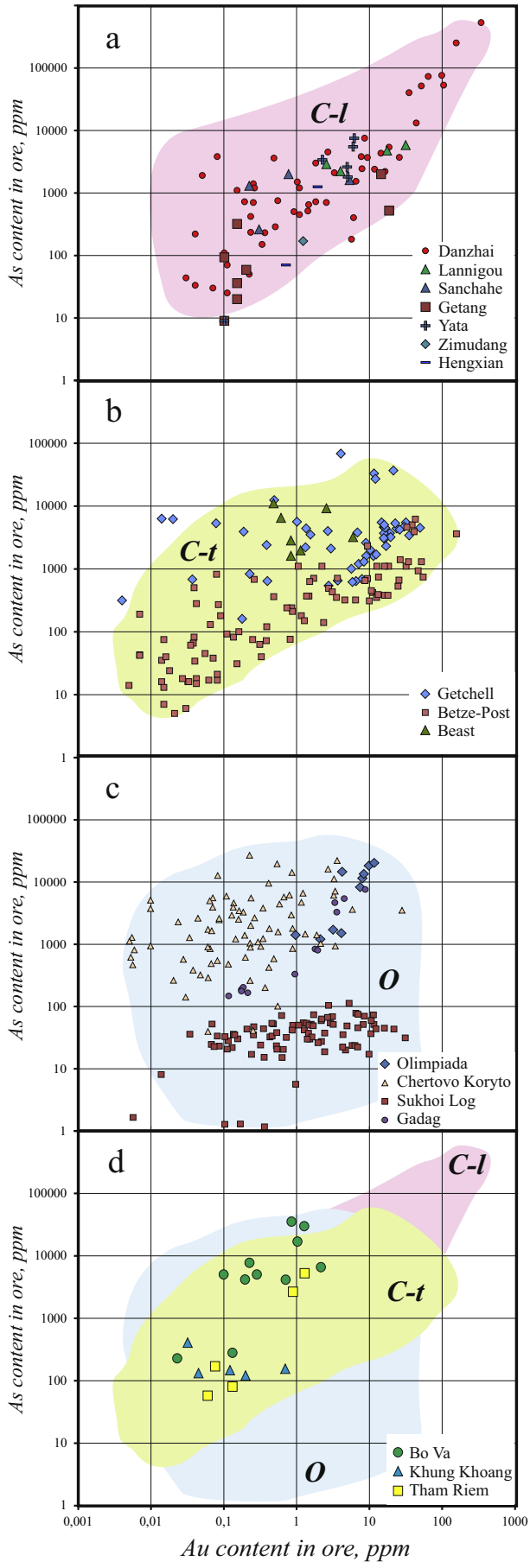

Fig. 6. Binary variation diagrams of Au vs. As in ore of Carlin-like deposit (China) (a), Carlin type deposits (Nevada, USA) (b), orogenic sedimentary rock-hosted gold deposits (c), and sedimentary rocks-hosted gold deposits in the Song Hien structure (d). These diagrams show that there is no difference between concentrations gold and arsenic. Data is for Danzhai (Lu, 1994), Yata, Getang, and Sanchahe (Ashley et al., 1991), Lannigou, Zimudang, and Hengxian (Peters, 2002), Getchell (Cail and Cline, 2001), Betze-Post (Kesler et al., 2003), Beast (Ressel et al., 2000), Chertovo Koryto and Sukhoi Log (Yudovskaya et al., 2016), Gadag (Ugarkar et al., 2016), Olimpiada (author's unpublished data).

Table 4
Sulfur isotope compositions of arsenopyrites and pyrites from Bo Va, Tham Riem and Khung Khoang gold deposits.

Deposit	Samp. No	Mineral	d34SV-CDT‰
Bo Va	KC14-3/1	Arsenopyrite	−6
	KC14-8/3	Arsenopyrite	−3.6
	KC14-307	Arsenopyrite	−5.1
	KC14-405	Arsenopyrite	−4.9
	KC14-407/1	Arsenopyrite	−3.2
	KC14-407/2	Arsenopyrite	−6.3
	KC14-414	Arsenopyrite	−7.1
	KC14-424	Arsenopyrite	−5.9
	KC14-433	Arsenopyrite	−7.4
	KC14-407/1	Pyrite	−6.1
	KC14-408	Pyrite	−3.7
	KC14-414	Pyrite	−5.8
	KC14-419	Pyrite	−7.4
	KC14-424	Pyrite	−4.2
Tham Riem	KC14-13/4	Arsenopyrite	−3.5
	KC14-476/1	Pyrite	−6.9
	KC14-476/2	Pyrite	−6.6
Khung Khoang	KC14-475/2	Pyrite	20.2
	KC14-475/5	Pyrite	20.2
	KC14-475/4	Pyrite	18.9
Host rock	KC14-477/1	Diagenetic pyrite	−17.7
	KC14-477/2	Diagenetic pyrite	−17.2

Note: (1) All values are reported as standard $d^{34}S$ notation relative to Canyon Diablo Troilite (V-CDT); (2) analytical uncertainty is within ±0.2‰; (3) host rock – black shale from outcrop near the Tham Riem deposit (see location sample in Fig. 3).

The geochemical signature of quartz veins is determined by high concentrations of Cu (up to 700 ppm), Zn (up to 2900 ppm), Cd (up to 10 ppm), Sb (up to 500 ppm), Pb (up to 545 ppm). The arsenic content in quartz veins is insignificant: not more than 130 ppm. Gold is present in quartz veins with tetrahedrite – sphalerite mineralization in the amount up to 0.13 ppm; The Au/Ag ratio increases to 10 (Table 3).

5.3. Sulfur isotopic composition

The sulfur isotopic composition of pyrite and arsenopyrite are presented in Table 4.

The isotopic compositions of pyrite and arsenopyrite from three areas within the Bo Va deposit are very similar and fall within a narrow range −3.2‰ to 7.4‰. Insignificant variations of the isotopic composition in sulfides (within 3‰) are independent of the level of gold content in the ores.

The isotopic compositions of pyrite and arsenopyrite in the Tham Riem deposit are close to that for the ores of the Bo Va deposit. The $\delta^{34}S$ values for pyrite are −6.6‰ and −6.9‰, for arsenopyrite −3.5‰.

At the same time, $\delta^{34}S$ of pyrite in the ores from the Khung Khoang deposit differs substantially towards much heavier isotopic composition showing the value +18.9 to +20.2‰.This isotopic composition is characteristic of pyrite from sulfidized shales with different gold content.

To estimate fractionation degree and determine sulfur sources for ores in the deposits, the isotopic composition of pyrite from host carbonaceous shales was determinated. The samples were

collected at a distance of about 1 km from ore bodies; they are carbonaceous shales with layers containing fine-grained pyrite. The layers enriched with sulfides follow the general folded patterns of host rocks. According to the results of ICP analysis, the gold content in these sulfidized shales is 61 ppb. The isotopic composition of pyrite is characterized by a light sulfur isotope: −17.2‰ and −17.7‰.

Therefore, in spite of the spatial closeness, mineralization at the Khung Khoang and Tham Riem deposits is characterized by substantial differences in the isotopic composition of sulfur in major sulfide minerals. At the same time, the isotopic composition of ores from the Tham Riem deposit corresponds to that of ores from the Bo Va deposit.

6. Discussion

6.1. Possible epigenetic process?

The mineral composition of ores from the studied deposits is rather simple and represents a typical set of minerals for this kind of mineralization (Novozhilov and Gavrilov, 1999; Konstantinov et al., 2009). On the one hand, there are a number of specific features in the mineral composition that distinguish the ores found in these deposits. The presence of arsenopyrite and pyrite in the form of coarse (up to 1–2 cm in size) crystals in the carbonaceous shale, the existence of micro-inclusions of chalcopyrite, sphalerite and native gold, and the low gold content in the sulfides themselves suggests the occurrence of superimposed processes entailing recrystallization of early gold-bearing sulfides. This mechanism of the formation of coarse metacrystals of low-gold pyrite with inclusions of native gold has been described in detail by Large et al. (2007) for the Suhoi Log gold deposit (Russia), for example. In addition, it was demonstrated in detail in a number of subsequent studies (Chang et al., 2008; Large et al., 2009, 2011) that the multistage formation of gold deposits involves gradual replacement of impurity-rich diagenetic pyrite by idiomorphic grains with mineral micro-inclusions of other sulfides and release of native gold.

The proposed mechanism for the changes of early gold-bearing sulfides is in agreement with the data we have presented and can explain a number of the features of the mineral occurrence: coarse idiomorphic grains of arsenopyrite; the absence of needle-like arsenopyrite; large amounts of chalcopyrite and sphalerite inclusions in pyrite and arsenopyrite; the absence of trace elements in pyrite and arsenopyrite; the low gold content of iron sulfides; and the occurrence of native gold. The broad occurrence of porphyroblasts of iron carbonate can also be a sign of the metamorphic reworking of ores (Large et al., 2007). As such, our studies allow us to assume the existence of superimposed metamorphic processes related to the complex history of the region.

6.2. Geochemical comparison with the Carlin-like gold deposits in the Yunnan–Guizhou–Guangxi "golden triangle" of southwestern China

The mineralogical and geochemical characteristics of the gold deposits in the Song Hien rift presented above allow us to divide them into two geochemical types. The first type includes the Bo Va and Tham Riem deposits and is characterized by high arsenic concentrations, as well as a relative enrichment in mercury and antimony. The second type is represented by the Khung Khoang deposit and is distinguished by substantially lower concentrations of arsenic in the ores (by almost one order of magnitude), with the other geochemical characteristics being the same.

To analyze the levels of enrichment, diagrams showing the concentrations of the most characteristic elements with respect to their clarke values are shown in Fig. 7 in which the coefficients of the Tl, Hg, Sb, As, Au, Ag, Pb, Zn, Cu, Mo and W concentrations are taken in consideration.

The deposits of the gold-arsenic geochemical profile demonstrate enrichment with arsenic within the range of 100–10,000 times with respect to the clarke level (clark values by Taylor, 1964). The relative concentrations of silver are not high; the silver content is increased by an order of magnitude. The ores are relatively enriched with antimony and to a lesser extent with mercury, while the concentrations of Tl and the basic metals (Pb, Z, and Cu)

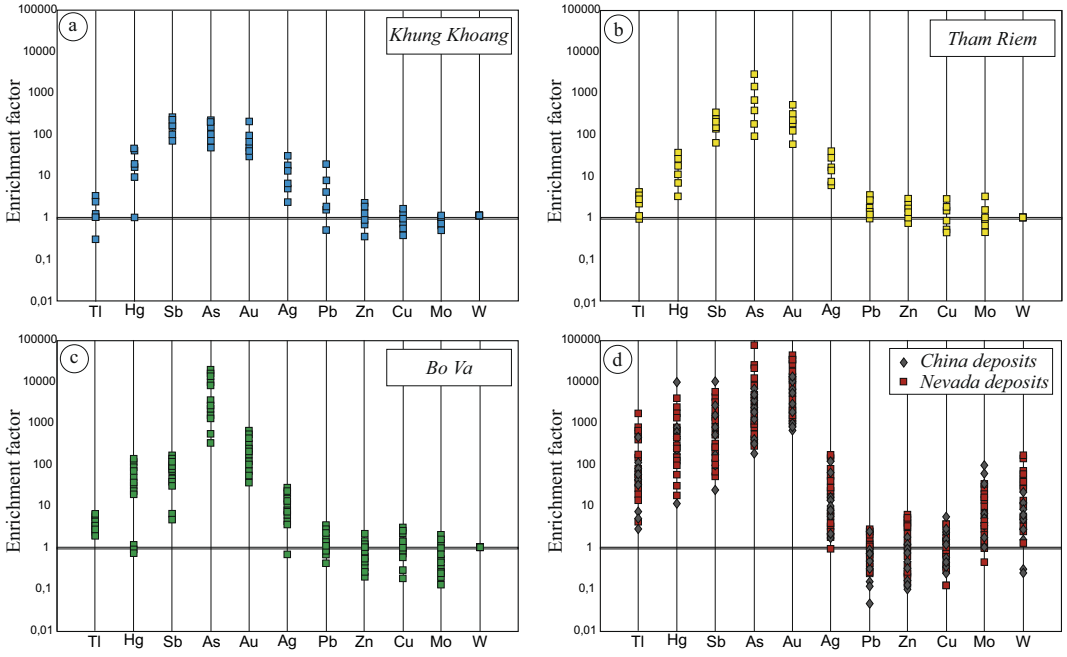

Fig. 7. Element enrichments in: a) Khung Khoang deposit; b) Tham Riem deposit; c) Bo Va deposit; d) 8 Yunnan–Guizhou–Guangxi "Golden Triangle" area deposits (gray diamonds) and 27 Nevada deposits (red squares) (data from Ashley et al., 1991; Lu, 1994; Peters, 2002; Zhang et al., 2005). (For interpretation of the references to colour in this figure legend, the reader is referred to the web version of this article.)

are at the clarke level or exceed it by less than an order of magnitude.

A somewhat different pattern of relative enrichment in the characteristic elements is noted in the ores from the Khung Khoang deposit. Of course, their enrichment in arsenic is observed but it is one or two orders of magnitude lower than that for the ores of the gold-arsenic type. In addition, the ores of the Khung Khoang deposit are characterized by a lower gold content, which is also seen in the plots. Thallium, zinc, and copper do not demonstrate significant enrichment. Lead concentrations, though not high, are increased with respect to the clarke level by an order of magnitude.

Analysis of the data obtained makes it evident that, in spite of their spatial association, the geochemical signature of the Khung Khoang and Tham Riem deposits differ in terms of their concentrations of arsenic, gold and, to a smaller extent, lead.

The most consistent anomalies in the carbonaceous sedimentary rock-hosted deposits are reflected by their elevated As, Cu, Zn, Cr, W, Ni, V, Pb, Sb, Bi, Te and Mo. A similar set of trace elements, As, Zn, V, Sb, Cr, Sn, Ni, Cu, Te, Mo, Pb, Hg, W and Tl, is inherent to Carlin type deposits (Large et al., 2011; Zhang et al., 2005). The concentration of gold and arsenic in the Carlin gold deposits in Nevada, the Carlin-like deposits in China, and orogenic sedimentary rocks-hosted gold deposits are at similar levels (Fig. 6). Though the majority of these elements are frequently found in increased concentrations in carbonaceous shales, it may be concluded by relying on the data from previous studies that one of the major differences in the geochemical features of Carlin type deposits relative to orogenic sedimentary rocks-hosted deposits is the enrichment of the former in Tl, Hg and to some extent in Sb.

The concentration coefficients for ores from different Carlin type deposits in Nevada and China are shown in the plot (Fig. 7d) (Zhang et al., 2005 and references therein). This plot shows the complete convergence of geochemical characteristics and therefore closeness of the sources of ore components for the deposits of the two gold ore provinces on a global scale. It is evident that the Carlin type deposits of both these gold ore provinces are characterized by substantial enrichment in Tl, Hg, Sb and, to a smaller extent, Mo and W.

Comparing the obtained data and the published ore geochemical data from Carlin type deposits, one may state that the gold deposits in black shales in northern Vietnam are characterized by a set of trace elements that does not correspond to that seen in the gold ore deposits of the Golden Triangle of south-western China. The set of trace elements in the ores of the studied deposits most likely corresponds to the ores found in the classic orogenic gold deposits in carbonaceous rocks (Fig. 6) (Goldfarb and Groves, 2015; Goldfarb et al., 2005; Groves et al., 1998; Novozhilov and Gavrilov, 1999; Yudovskaya et al., 2016).

6.3. Possible origins of sulfur

Gold in orogenic gold deposits is transported mainly in the form of sulfide complexes (Goldfarb et al., 2005; Groves et al., 2003), therefore the investigation of sulfur sources is very important to understand the sources of gold, hydrothermal fluids and ore genesis in general (Chang et al., 2008; Chai et al., 2016). We studied the isotopic composition of sulfur in pyrite and arsenopyrite which are the major sulfide minerals of the gold mineralization herein studied. The results reported above allow us to make the following conclusions.

The isotopic compositions of pyrite and arsenopyrite in the ores from three areas within the Bo Va deposit lie within the narrow range −3.5 to −7.4‰. The isotopic compositions of pyrite and arsenopyrite in the ores from the Tham Riem deposit lie within the same range −3.5 to −6.6‰. This may be evidence of common

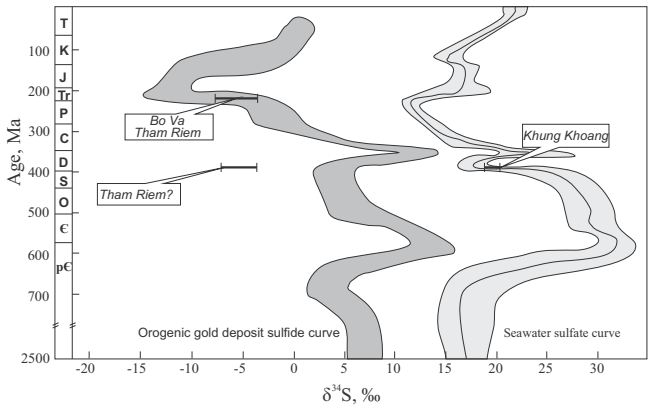

Fig. 8. Variation of sulfide S isotopic compositions in sedimentary rocks-hosted orogenic gold deposits through geologic time and seawater sulfate curve. Figure shows that the variation in S isotope compositions of the deposits through geologic time has a pattern similar to the seawater sulfate curve. The $\delta^{34}S$ values of the sulfides are typically ~15‰ to 20‰ lighter than the coeval seawater sulfate, though the difference can be smaller (~10‰) or larger (~30‰) (Chang et al., 2008).

sources of sulfur and the ore components during the formation of the mineralization.

The narrow range of the sulfur isotopic compositions of the major ore minerals (within 3‰) indirectly confirms the assumption concerning the existence of epigenetic overprinting of gold ores. Homogenization of the isotopic system of sulfur in the case of superposition of metamorphic processes has been demonstrated in detail by Large et al. (2007) and Chang et al. (2008).

The sulfur isotopic composition in pyrite of the Khung Khoang ores demonstrates substantial enrichment with heavy sulfur – +20‰. This isotopic composition of sulfur allows to state that its source is primarily different from that of the Bo Va and Tham Riem deposits.

The isotopic composition of sulfur in pyrite and arsenopyrite in ores from the Tham Riem and Bo Va deposits shown in Fig. 8, corresponds to that for gold deposits located in Triassic sedimentary rocks. This confirms that the source of sulfur and possibly other ore components was the host rocks without any participation of magmatic fluid (Large et al., 2007).

The isotopic composition of sulfur in pyrite of the ores from the Khung Khoang deposit corresponds closely to the isotopic composition of marine sulfates formed during the Devonian age (Fig. 8).

Study of the isotopic composition of sulfur in major ore minerals allows us to validate different sources of sulfur and ore components for the gold deposits of northeastern Vietnam. The source of sulfur for the formation of the stratiform gold-pyrite type Khung Khoang deposit was the sedimentary rocks of the Lower Devonian Mia Le formation, which is composed mainly of black shale and, marly shale with lesser amounts of limestone. Hydrothermal-metamorphogenic fluids derived sulfur from sulfate within the carbonate sequences. Sulfur from marine sulfate enriched with the heavy isotope was later reduced through the participation of the organic matter with which the carbonaceous shale is saturated (Seal, 2006).

6.4. A Devonian or Triassic host rock for the Tham Riem deposit?

According to geological maps of different scales (DGMV, 1997, 2000), the Tham Riem deposit are hosted in the sedimentary rocks of the Mia Le formation of the Lower Devonian. However, the results of our studies allow us to assume that the host rocks for this deposit are represented by the black shale rocks of the Song Hien formation of the Lower Triassic. The deposit is spatially confined to the coupling zone between two regional-scale structures (the Song Hien rift and the adjacent Lo Gam fold belt), therefore we

suppose that the tectonic blocks include both Devonian and Triassic sedimentary rocks.

The spatial closeness of the Tham Riem and Khung Khoang deposits should lead us to assume that the host rocks are represented by a single sedimentary unit. However, the results of our studies demonstrated substantially different mineral compositions, different levels of gold content in the ores, different geochemical patterns of mineralization, and significant differences in the isotopic composition of sulfur. All the listed characteristics for the Tham Riem deposit correspond to those of the Bo Va deposit, which is hosted in the terrigenous sedimentary rocks of the Lower Triassic Song Hien formation.

Therefore, we assume that the host rocks for the ores of the Tham Riem deposit are represented by Lower Triassic black shales. Taking into account the position of the Nam Quang ore cluster (to which the Tham Riem and Khung Khoang deposits belong) in a tectonically deformed block, the existence of separate blocks of Lower Triassic rocks appears very plausible. The petrographic composition of the carbonaceous shale of the Mia Le formation of the Lower Devonian and the Song Hien formation of the Lower Triassic is very similar (Thanh and Khuc, 2006), and the two units are not always clearly distinguished.

6.5. Possible genetic model for the Au deposits in the Song Hien structure, Northeastern Vietnam

Based on the obtained data, and the published studies on Carlin-like deposits in southern China, we conclude that the formation of the Bo Va, Tham Riem and Khung Khoang gold deposits is related to the development of the Song Hien rift basin. Several stages of metallogenic development may be distinguished in the long history of formation of these deposits.

The first stage is linked to the formation of a rift system with tectono-magmatic processes related to the Emeishan LIP. The Song Hien rift was characterized by intense subaqueous volcanism (rhyolite fields and pillow basaltic lavas), as well as by numerous manifestations of mafic-ultramafic magmatism, at the end of the Permian and the beginning of Triassic (Hoa et al., 2008; Izokh et al., 2005; Polyakov et al., 2009). The ages of lherzolite and gabbrodolerite (262–266 Ma) and rhyolite (248 Ma) from the Song Hien rift have been determined by Hoa et al. (2008, 2016). We argue that these processes could lead to the primary enrichment in gold of the sediments of the rift basin. At that time, the Song Hien formation of the Lower Triassic was formed. The rocks of this formation were enriched in organic matter, sulfur, arsenic and

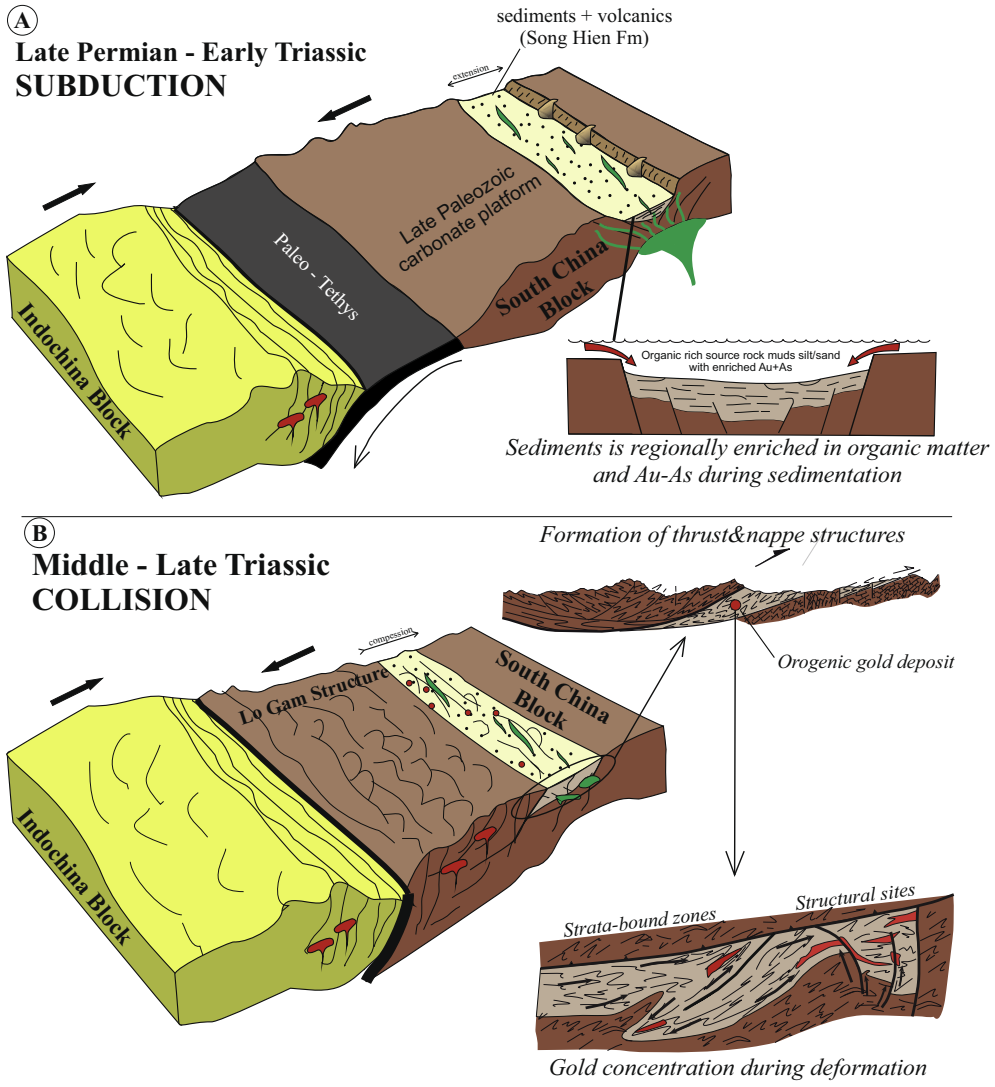

Fig. 9. Proposed conceptual model for formation sedimentary rock-hosted gold deposits in the Song Hien structure. See text for explanation. The model is schematic and not to scale and is only designed to provide a holistic view. Data and idea for figure from Faure et al., 2014; Hoa et al., 2008; Hu et al., 2014; Large et al., 2011; Lepvrier et al., 2011; Liu et al., 2012; Pirajno and Bagas, 2008.

gold, leading to the development of the source ore-bearing sedimentary rocks occurred (Fig. 9A).

The second stage of the development of the Song Hien rift basin was related to the beginning of the collision between the Indochina and South China Blocks in the Middle Triassic (Faure et al., 2014; Lepvrier et al., 1997, 2008, 2011; Liu et al., 2012). Extensional processes in the rift structure changed to compression processes, resulting in the decay of the magmatic activity. At this time, thick sequences of turbidite were formed (Faure et al., 2014; Lepvrier et al., 2011; Tri and Vu, 2011). As a result of the considerable increase in the thickness of sedimentary rocks, dehydration of Lower Triassic lithologies began. Primary metamorphic fluids formed and became enriched with ore components leached out of host rocks by fluid-rock interactions. These metamorphic fluids became concentrated in various structural settings, for example, in the cores of anticlinal folded structures (Fig. 9B).

The final stage of the development of Song Hien structure is related to the collision between Indochina and South China Blocks in the Middle and Late Triassic (Faure et al., 2014) and to the formation of thrust and nappe structures (Lepvrier et al., 2011). During this stage, the sedimentary rocks of the Song Hien rift basin were subjected to maximal compression (Faure et al., 2014). Buried metal-bearing metamorphic fluids escaped from structural traps and flowed along fracture structures to zones of lower pressure. Migration of metal-bearing solutions was accompanied by their enrichment in ore components due to extraction from host rocks by fluid-rock interaction. The formation of gold mineralization proceeded during the change in physicochemical parameters, fluid mixing with meteoric water, extensive changes in the chemical composition of host rocks, and decreases in pressure (at the boundaries of lithologic, structural unconformities and fracture zones) (Fig. 9B).

In addition, our studies allowed us to infer the activity of later processes that led to local redistribution of the ore components within the deposit, as well as recrystallization and release of gold as a separate mineral phase. Similar processes nave been described in detail by Large et al. (2007).

This model describes the formation of gold mineralization of the arsenic type that is hosted in Triassic sedimentary rocks within the Song Hien rift structure. For the ores of the Khung Khoang deposit hosted in Devonian sedimentary rocks, we propose another model, though somewhat similar processes that led to the formation of economic gold ores. The differences include (i) the formation of the source ore-bearing layer proceeded in different settings, given the dominant carbonate accumulation during the Devonian (which produced the different geochemical signature of the deposit and significant differences in the isotopic composition of sulfur). Also, (ii) the metal-bearing metamorphic fluids migrated within the same layer, leading to local enrichment and redistribution of the ore components. As a consequence, the mineralization has a stratiform appearance, and the ore bodies are concordant with the stratification of the host rocks. This model explains the important differences in the geochemical, mineralogical and isotopic signatures of this deposit.

In spite of the above-mentioned differences in the mineral composition and geochemical features of the ores in the deposits of Northeastern Vietnam and those of south-western China, we assume a unified history of formation and association with tectonic events in the region. The differences between the two districts may be due to different conditions of sedimentation in the Triassic-age Song Hien and Nanpanjang rift troughs, which are found in Vietnam and in China, respectively. In the latter, a more important role in the Triassic section is played by carbonate and terrigenous-carbonate sedimentary rocks (Peters et al., 2007), while terrigenous and terrigenous-volcanogenic sedimentary rocks are more strongly developed in Vietnam. In addition, the formation of mineralization could be affected by the degree of manifestation of tectonic processes; hence, the mineralization temperatures might have been different.

The time of formation of Carlin-like gold deposits in Southern China is 235–193 Ma, on the basis of results from the re-Os, Rb-Sr and Ar-Ar methods (Chen et al., 2015a; Gu et al., 2012; Su et al., 2009). The Carlin-like deposits in the Yunnan–Guizhou–Guangxi area formed under a post-collision transpressional regime during the Late Triassic to Early Jurassic period (Chen et al., 2015a). The Song Hien structure was exposed to the same tectonic processes during the amalgamation of South China with Indochina (Faure et al., 2014; Lepvrier et al., 2011) that produced the Nanpanjang basin. Using the principle of Occam's razor, which states that the hypothesis with the least number of assumptions is the best, the simplest and most elegant model is that the formation of sedimentary rocks-hosted gold deposit in the Song Hien structure may be related to the Indosinian Orogeny. Nevertheless, we conclude that the gold deposits of northern Vietnam and southwestern China formed within the same tectonic stage. The proposed model of the formation of gold deposits in North-Eastern Vietnam allows us to assume that the age of this mineralization coincides with that of post-orogenic tectonic processes (225–205 Ma) (Faure et al., 2014).

7. Conclusion

Based on the mineral composition of their ores, the studied deposits were divided into two types, which are the (i) pyrite and (ii) pyrite-arsenopyrite types. The first type includes the ores of the Khung Khoang deposit. In this deposit, pyrite is the only ore mineral. The Bo Va and Tham Riem deposits belong to the pyrite-arsenopyrite type. The ores of these deposits are characterized by extensive impregnation with coarse idiomorphic grains of pyrite and arsenopyrite. The quantitative relations between the two major ore minerals vary within the limits of each ore body but remain constant on the deposit scale.

The formation of these deposits is most likely related to the Indosinian orogenies, which included the formation of a series of thrust faults, regional metamorphism and deformation of the terrigenous sedimentary rocks of the Song Hien rift. These deposits differ in terms of their mineral compositions and geochemical features of their ores compared to the deposits of the Chinese Golden Triangle and are representative of orogenic gold deposits in carbonaceous sedimentary rocks.

The narrow range of variation in the sulfur isotopic compositions of pyrite and arsenopyrite; the presence of visible gold as inclusions; the presence of chalcopyrite, sphalerite and other inclusions in arsenopyrite and pyrite; and the large size of the grains of major ore minerals allow us to assume that the primary gold ores of the Bo Va and Tham Riem deposits underwent epigenetic reworking.

The absence of the trace elements including arsenic, antimony, mercury and other characteristic elements from the ores of the Khung Khoang deposit and the substantially heavier isotopic composition of sulfur, which corresponds to the isotopic composition of sulfur in marine sulfates during the Devonian, allow us to infer another source of the ore components that was not connected with the sedimentary rocks of the Song Hien rift.

Acknowledgments

The constructive comments and careful revisions from Franco Pirajno, Editor-in Chief of Ore Geology Reviews, and two reviewers are greatly appreciated. We sincerely thank Alexander S. Borisenko for the extensive reviews of our manuscript. The work was

supported by the Project KC08.14/11-15 of MOST of Vietnam, the Grant of President Russian Federation (MK-7305.2016.5), and partially by state assignment projects of IGM SB RAS (VIII.72).

References

Anh, Tran Tuan, Gaskov, I.V., Hoa, Tran Trong, Borisenko, A.S., Izokh, A.E., Pham, Thi Dung, Ly, Vu Hoang, Nguyen, Thi Mai, 2015. Ta Nang gold deposit in the black shales of Central Vietnam. Russ. Geol. Geophys. 56, 1414–1427.

Ashley, R.P., Cunningham, C.G., Bostick, N.H., Dean, W.E., Chou, I.M., 1991. Geology and geochemistry of three sedimentary rock-hosted disseminated gold deposits in Guizhou province, People's Republic of China. Ore Geol. Rev. 6, 133–151.

Berger, V.I., Mosier, D.L., Bliss, J.D., Moring, B.C., 2014. Sediment-hosted gold deposits of the world—database and grade and tonnage models (ver. 1.1, June 2014): U.S. Geological Survey Open-File Report 2014–1074, doi:10.3133/ofr20141074.

Cai, J., Xiaodong, T., Yi, W., 2014. Magnetic fabric and paleomagnetism of the Middle Triassic siliciclastic rocks from the Nanpanjiang Basin, South China: implications for sediment provenance and tectonic process. J. Asian Earth Sci. 80, 134–147.

Cail, T.L., Cline, J.S., 2001. Alteration associated with gold deposition at the Getchell Carlin-type gold deposit, north-central Nevada. Econ. Geol. 96, 1343–1359.

Chai, P., Sun, J.G., Hou, Z.Q., Xing, S.W., Wang, Z.Y., 2016. Geological, fluid inclusion, H–O–S–Pb isotope, and Ar–Ar geochronology constraints on the genesis of the Nancha gold deposit, southern Jilin Province, northeast China. Ore Geol. Rev. 72, 1053–1071.

Chang, Z., Large, R.R., Maslennikov, V., 2008. Sulfur isotopes in sediment-hosted orogenic gold deposits: evidence for an early timing and a seawater sulfur source. Geology 36, 971–974.

Chen, M.H., Mao, J.W., Bierlein, F.P., Norman, T., Uttley, P.J., 2011. Structural features and metallogenesis of the Carlin-type Lannigou gold deposit, Guizhou Province, China. Ore Geol. Rev. 43, 217–234.

Chen, Z., Lin, W., Faure, M., Lepvrier, C., Nguyen, V.V., Vu, V.T., 2014. Geochronology and isotope analysis of the Late Paleozoic to Mesozoic granitoids from northeastern Vietnam and implications for the evolution of the South China block. J. Asian Earth Sci. 86, 131–150.

Chen, M., Mao, J., Chao, L., Zhang, Z., Dang, Y., 2015a. Re–Os isochron ages for arsenopyrite from Carlin-like gold deposits in the Yunnan–Guizhou–Guangxi "golden triangle", southwestern China. Ore Geol. Rev. 64, 316–327.

Chen, M., Zhang, Z., Santosh, M., Dang, Y., Zhang, W., 2015b. The Carlin-type gold deposits of the "golden triangle" of SW China: Pb and S isotopic constraints for the ore genesis. J. Asian Earth Sci. 103, 115–128.

DGMV, 1997. Geological map (F-48-43-b): 1:50,000 scale.

DGMV, 2000. Geological Map of Bao Lac (F-48-X): 1:200,000 scale.

Faure, M., Lepvrier, C., Nguyen, V.V., Vu, T.V., Lin, W., Chen, Z., 2014. The South China block-Indochina collision: where, when, and how? J. Asian Earth Sci. 79, 260–274.

Galfetti, T., Bucher, H., Martini, R., Hochuli, P., Weissert, H., Crasquin-Soleau, S., Brayard, A., Goudemand, N., Brühwiler, T., Guodun, K., 2008. Evolution of Early Triassic outer platform paleoenvironments in the Nanpanjiang basin (South China) and their significance for the biotic recovery. Sediment. Geol. 204, 36–60.

Gold deposits of Russia, 2010. Konstantinov, M.M. (Ed.). Moscow. (in Russian).

Goldfarb, R.J., Groves, D.I., 2015. Orogenic gold: common or evolving fluid and metal sources through time. Lithos 233, 2–26.

Goldfarb, R.J., Baker, T., Dube, B., Groves, D.I., Hart, C.J.R., Gosselin, R., 2005. Distribution, character, and genesis of gold deposits in metamorphic terranes. In: Hedenquist, J.W. et al. (Eds.), Economic Geology 100th Anniversary Volume: Littleton, Colorado, Econ. Geol., pp. 407–450.

Goldfarb, R.J., Taylor, R.D., Collins, G.S., Goryachev, N.A., Orlandini, O.F., 2014. Phanerozoic continental growth and gold metallogeny of Asia. Gondwana Res. 25, 48–102.

Goryachev, N.A., 2006. Gold ore forming systems of orogenic belts. Vestnik NESC FEB RAS, 1, 2–16 (in Russian).

Goryachev, N.A., Yakubchuk, A., 2008. Gold deposits of Magadan region, northeastern Russia: yesterday, today, and tomorrow. SEG Newsletter 74 (1), 9–15.

Groves, D.I., Goldfarb, R.J., Gebre-Mariam, M., Hagemann, S.G., Robert, F., 1998. Orogenic gold deposits—a proposed classification in the context of their crustal distribution and relationship to other gold deposit types. Ore Geol. Rev. 13, 7–27.

Groves, D.I., Goldfarb, R.J., Robert, F., Hart, C.J.R., 2003. Gold deposits in metamorphic belts: overview of current understanding, outstanding problems, future research, and exploration significance. Econ. Geol. 98, 1–29.

Gu, X.X., Zhang, Y.M., Li, B.H., Dong, S.Y., Xue, C.J., Fu, S.H., 2012. Hydrocarbon- and ore-bearing basinal fluids: a possible link between gold mineralization and hydrocarbon accumulation in the Youjiang basin, South China. Mineral. Deposita 47, 663–682.

Guangxi BGMR (Bureau of Geology and Mineral Resources), 1985. Regional Geology of Guangxi Zhuang Autonomous Region. Geological Memoirs, Series 1, 3, pp. 853.

Han, L., Tanweer, A., Szaran, J., Halas, S., 2002. A modified technique for the preparation of SO_2 from sulphates and sulphides for sulfur isotope analyses. Isot. Environ. Health Stud. 38, 177–183.

Hoa, T.T., 2007. Intraplate magmatism of Northern Vietnam and Metallogeny. Dr. of Sci. Dissertation, VS Sobolev Institute of Geology and Mineralogy SB RAS, Novosibirsk (in Russian).

Hoa, T.T., Tran, T.A., Ngo, T.P., Izokh, A.E., Polyakov, G.V., Balykin, P.A., Ching-Ying, L., Hoang, H.T., Bui, A.N., Pham, T.D., 2004. Gabbro-syenite associations of East Bac Bo structures: evidences of intra-plate magmatism? J. Geol. Ser. B 23, 12–25.

Hoa, T.T., Izokh, A.E., Polyakov, G.V., Borisenko, A.S., Anh, T.T., Balykin, P.A., Phuong, N.T., Rudnev, S.N., Van, V.V., Nien, B.A., 2008. Permo-Triassic magmatism and metallogeny of Northern Vietnam in relation to the Emeishan plume. Russ. Geol. Geophys. 49, 480–491.

Hu, L., Du, Y., Cawood, P.A., Xu, Y., Yu, W., Zhu, Y., Yang, J., 2014. Drivers for late Paleozoic to early Mesozoic orogenesis in South China: constraints from the sedimentary record. Tectonophysics 618, 107–120.

Ishihara, S., Pham, T.X., 2013. Distribution of some ore metals around the Mau Due stibnite deposits, northernmost Vietnam. Bull. Geol. Surv. Jpn. 64 (1/2), 51–57.

Izokh, A.E., Polyakov, G.V., Hoa, T.T., Balykin, P.A., Phuong, N.T., 2005. Permian-Triassic ultramafic–mafic magmatism of Northern Vietnam and Southern China as expression of plume magmatism. Russ. Geol. Geophys. 46, 942–951 (in Russian).

Kesler, S.E., Fortuna, J., Ye, Z., Alt, J.C., Core, D.P., Zohar, P., Borhauer, J., Chryssoulis, S. L., 2003. Evaluation of the role of sulfidation in deposition of gold, Screamer Section of the Betze-Post Carlin-type deposit, Nevada. Econ. Geol. 98, 1137–1157.

Konstantinov, M.M., Nekrasov, E.M., Sidorov, A.A., Struzhkov, S.F., 2009. Gold-Ore Giants of Russia and the World. Nauchnyi Mir, Moscow (in Russian).

Large, R.R., Maslennikov, V.V., Robert, F., Danyushevsky, L.V., Scott, R.J., Chang, Z., 2007. Multi-stage sedimentary and metamorphic origin of pyrite and gold in the giant Sukhoi Log deposit, Lena Goldfi eld, Russia. Econ. Geol. 102, 1233–1267.

Large, R.R., Danyushevsky, L., Hollit, C., Maslennikov, V., Meffre, S., Gilbert, S., Bull, S., Scott, R., Emsbo, P., Thomas, H., Singh, B., Foster, J., 2009. Gold and trace element zonation in pyrite using a laser imaging technique; implications for the timing of gold in orogenic and carlin-style sediment-hosted deposits. Econ. Geol. 104, 635–668.

Large, R.R., Stuart, W., Maslennikov, V.V., 2011. A carbonaceous sedimentary source-rock model for carlin-type and orogenic gold deposits. Econ. Geol. 106, 331–358.

Leloup, P.H., Lacassin, R., Tapponnier, P., Schärer, U., Zhong, D., Liu, X., Zhang, L., Ji, S., Trinh, P., 1995. The Ailaoshan-Red River shear zone (Yunnan, China), Tertiary transform boundary of Indochina. Tectonophysics 252, 3–84.

Lepvrier, C., Maluski, H., Voung, N.V., Roques, D., Axente, V., Rangin, C., 1997. Indosinian NW-trending shear zones within the Truong Son belt (Vietnam): $^{40}Ar–^{39}Ar$ Triassic ages and Cretaceous to Cenozoic overprints. Tectonophysics 283, 105–127.

Lepvrier, C., Vuong, N.V., Maluski, H., Thi, P.T., Tich, V.V., 2008. Indosinian tectonics in Vietnam. C.R. Geosci. 340, 94–111.

Lepvrier, C., Faure, M., Voung, N.V., Tich, V.V., Lin, W., Thang, T.T., Phuong, T.H., 2011. North-directed Triassic nappes in Northeastern Vietnam (East Bac Bo). J. Asian Earth Sci. 41, 56–68.

Liu, J., Tran, M., Tang, Y., Nguyen, Q.L., Tran, T.H., Wu, W., Chen, J., Zhang, Z., Zhao, Z., 2012. Permo-Triassic granitoids in the northern part of the Truong Son belt, NW Vietnam: geochronology, geochemistry and tectonic implications. Gondwana Res. 122, 628–644.

Lu, G.Q., 1994. A Genetic Link Between the Gold-Mercury Mineralization and Petroleum Evolution – A Case of the Danzhai Gold-Mercury Deposit (PhD thesis). Universite du Quebec, Chicoutimi, Quebec.

Morelli, R., Creaser, R.A., Seltmann, R., Stuart, F.M., Selby, D., Graupner, T., 2007. Age and source constraints for the giant Murunatu gold deposit, Uzbekistan, from coupled Re–Os–He isotopes in arsenopyrite. Geology 35, 795–798.

Nguyen, V.N., 2008. Formations of endogenous ore deposits and mineralization in Vietnam. VNU J. Sci. Earth Sci. 24, 26–31.

Novozhilov, Yu.I., Gavrilov, A.M., 1999. Gold-Sulfide Deposits in Carbonaceous Terrigenous Strata. TsNIGRI, Moscow (in Russian).

Nozhkin, A.D., Borisenko, A.S., Nevol'ko, P.A., 2011. Stages of Late Proterozoic magmatism and periods of Au mineralization in the Yenisei Ridge. Russ. Geol. Geophys. 52, 124–143.

Peng, Y., Xuexiang, G., Yongmei, Z., Li, L., Chengyun, W., Siyao, C., 2014. Ore-forming process of the Huijiabao gold district, southwestern Guizhou Province, China: evidence from fluid inclusions and stable isotopes. J. Asian Earth Sci. 93, 89–101.

Peters, S.G., 2002. Geology, geochemistry, and geophysics of sedimentary-hosted Au deposits in P.R. China. U.S. Geological Survey Open-File Report, 02-131, Version 1.0, <http://geopubs.wr.usgs.gov/open-file/of02-131/>.

Peters, S.G., Huang, J.Z., Li, Z.P., Jing, C.G., 2007. Sedimentary rock-hosted Au deposits of the Dian–Qian–Gui area, Guizhou, and Yunnan Provinces, and Guangxi District, China. Ore Geol. Rev. 31, 170–204.

Petrov, V.G., Hoa, Tran Trong, Hoang, Huu Thanh, Ngo, Thi Phuong, Vu, Van Van, Tran, Quoc Hung, Bui, An Nien, Hoang, Viet Hang, 1996. Structure of ore fields of gold bearing quartz vein of Bo Va gold mine (Cao Bang). Geology – Resources. Pub. Sci. & Tec., vol. 1, pp. 361–367 (in Vietnamese).

Pirajno, F., Bagas, L., 2008. A review of Australia's Proterozoic mineral systems and genetic models. Precambr. Res. 166, 54–80.

Polyakov, G.V., Ngyen, T.Y., Balykin, P.A., Tran, T.H., Hoang, H.T., Tran, Q.H., Ngo, T.P., Petrova, T.E., Vu, V.V., 1996. Permian – Triassic mafic-ultramafic associations of Northern Vietnam. Hanoi. "Science and Technics" Publishing House (in Vietnamese).

Polyakov, G.V., Shelepaev, R.A., Hoa, T.T., Izokh, A.E., Balykin, P.A., Phuong, N.T., Hung, T.Q., Nien, B.A., 2009. The Nui Chua layered peridotitegabbro complex as manifestation of Permo-Triassicmantle plume in northern Vietnam. Russ. Geol. Geophys. 50, 501–516.

Ressel, M.W., Noble, D.C., Henry, C.D., Trudel, W.S., 2000. Dike-hosted ores of the Beast deposit and the importance of Eocene magmatism in gold mineralization of the Carlin Trend, Nevada. Econ. Geol. 95, 1417–1444.

Roger, F., Maluski, H., Lepvrier, C., Tich, V.V., Paquette, J.-L., 2012. LA-ICPMS zircons U/Pb dating of Permo-Triassic and Cretaceous magmatisms in Northern Vietnam – Geodynamical implications. J. Asian Earth Sci. 48, 72–82.

Seal, R.R., 2006. Sulfur isotope geochemistry of sulfide minerals. Rev. Mineral. Geochem. 61, 633–677.

Spiridonov, E.M., 1996. Granitic rocks and gold mineralization of north Kazakhstan. In: Shatov, V., Seltmann, R., Kremenetsky, A., Lehmann, B., Popov, V., Ermolov, P. (Eds.), Granite-Related Ore Deposits of Central Kazakhstan and Adjacent Areas. GLAGOL Publishing House, St. Petersburg, pp. 197–217.

Su, W.C., Heinrich, C.A., Pettke, T., Zhang, X.C., Hu, R.Z., Xia, B., 2009. Sediment-hosted gold deposits in Guizhou, China: products of wall-rock sulfidation by deep crustal fluids. Econ. Geol. 104, 73–93.

Svetlitskaya, T.V., Tolstykh, N.D., Izokh, A.E., Phuong, N.T., 2015. PGE geochemical constraints on the origin of the Ni-Cu-PGE sulfide mineralization in the Suoi Cun intrusion, Cao Bang province, Northeastern Vietnam. Mineral. Petrol. 109, 161–180.

Tapponnier, P., Lacassin, R., Leloup, H., Schärer, U., Zhong, D., Liu, X., Ji, S., Zhang, L., Zhong, J., 1990. The Ailaoshan-Red river metamorphic belt: tertiary left-lateral shear between Indochina and South China. Nature 343, 431–437.

Taylor, S.R., 1964. Abundance of chemical elements in the continental crust; a new table. Geochim. Cosmochim. Acta 28, 1273–1285.

Thanh, T.-Z., Khuc, V. (Eds.), 2006. Stratigraphic Units of Vietnam. Vietnam National University Publishing House, Hanoi.

Tran, T.H., Nevolko, P.A., Ngo, T.P., Svetlitskaya, T.V., Vu, H.L., Redin, Y., Tran, T.A., Pham, T.D., Ngo, T.H., 2016a. Geology, geochemistry and sulphur isotopes of the Hat Han gold-antimony deposit, NE Vietnam. Ore Geol. Rev. 78, 69–84.

Tran, T.H., Polyakov, G.V., Tran, T.A., Borisenko, A.S., Izokh, A.E., Balykin, P.A., Ngo, T. P., Pham, T.D., 2016b. Intraplate Magmatism and Metallogeny of North Vietnam. Modern Approaches in Solid Earth Sciences. Springer International Publishing House, Switzerland, p. 372.

Tri, T.V., Vu, K., 2011. Geology and Earth Resources of Vietnam. General Dept of Geology, and Minerals of Vietnam, Hanoi, Publishing House for Science and Technology.

Tyukova, Ye.E., Voroshin, S.V., 2007. Arsenopyrite Mineral Composition and Parageneses in Ore Deposit and Host Rocks Throughout the Upper Kolyma River Area (Interpreting the Genesis of Sulfide Mineral Assemblages). NEISRI FEB RAS, Magadan (in Russian).

Ugarkar, A.G., Malapur, M.A., Kumar, B.C., 2016. Archean turbidite hosted orogenic gold mineralization in the Gadag greenstone belt, Western Dharwar Craton, Peninsular India. Ore Geol. Rev. 72, 1224–1242.

Vladimirov, A.G., Balykin, P.A., Anh, P.L., Kruk, N.N., Phuong, N.T., Travin, A.V., Hoa, T. T., Annikova, I.Y., Kuybida, M.L., Borodina, E.V., Karmysheva, I.V., Nien, B.A., 2012. The Khao Que-Tam Tao gabbro-granite massif, Northern Vietnam: a petrological indicator of the Emeishan plume. Russ. J. Pacific Geol. 6, 395–411.

Yakubchuk, A., Cole, A., Seltmann, R., Shatov, V., 2002. Tectonic setting, characteristics, and regional exploration criteria for gold mineralization in the Altaid orogenic collage: the Tien Shan province as a key example. Soc. Econ. Geol. Spec. Publ. 9, 177–201.

Yang, J., Peter, A.C., Yuansheng, D., Hu, H., Huang, H., Ping, T., 2012. Large Igneous Province and magmatic arc sourced Permian-Triassic volcanogenic sediments in China. Sediment. Geol. 261–262, 120–131.

Yudovskaya, M.A., Distler, V.V., Prokofiev, V.Yu., Akinfiev, N.N., 2016. Gold mineralisation and orogenic metamorphism in the Lena province of Siberia as assessed from Chertovo Koryto and Sukhoi Log deposits. Geosci. Front. 7, 453–481.

Zeng, Y.F., Liu, W.J., Chen, H.D., Zheng, R.C., Zhang, J.Q., Li, X.Q., Jiang, T.C., 1995. Evolution of sedimentation and tectonics of the Youjiang composite basin, south China. Acta Geol. Sinica 69, 113–124 (in Chinese with English abstract).

Zhang, X.C., Hofstra, A.H., Hu, R.-Z., Emsbo, P., Su, W., Ridley, W.I., 2005. Geochemistry and ä34S of ores and ore stage iron sulfides in Carlin-type gold deposits, Dian-Qian-Gui area, China: Implications for ore genesis. In: Mao, J.W., Bierlein, F.P. (Eds.), Mineral Deposits Research: Meeting the Global Challenge, vol. 2, pp. 1107–1110.

Zhang, R.Y., Lo, C.H., Chung, S.L., Grove, M., Omori, S., Iizuka, Y., Liou, J.G., Tri, T.V., 2013. Origin and tectonic implication of ophiolite and eclogite in the Song Ma Suture Zone between the South China and Indochina Blocks. J. Metamorphic Geol. 31, 49–62.

Zhong, H.R., Chao, S.W., Wu, B.X., Zhi, T.G., Hofstra, A.H., 2002. Geology and geochemistry of Carlin-type gold deposits in China. Mineral. Deposita 37, 378–392.

Zhou, T.H., Goldfarb, R.J., Phillips, G.N., 2002. Tectonics and metallogeny of gold deposits in China. Mineral. Deposita 37, 249–282.